UNIVERSITY OF NAIROBI

DEVELOPMENT OF A DIFFERENTIAL NORMAL PULSE VOLTAMMETRIC METHOD FOR PHOSPHATE DETERMINATION IN WATER

BY

KINYANJUI WALLACE KARANJA

I56/12121/2018

A Thesis Submitted in Partial Fulfilment of the Requirements for the Award of the Degree of Master of Science in Analytical Chemistry of the University of Nairobi

2023

DECLARATION

I declare that this thesis is my original work and has not been submitted elsewhere for research. Where other people's work or my own work has been used, this has properly been acknowledged and referenced in accordance with the University of Nairobi's requirements.

Signature: …….   ………   Date: ……09/06/2023……

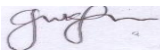**WALLACE KARANJA KINYANJUI**

156/12121/2018

DEPARTMENT OF CHEMISTRY

FACULTY OF SCIENCE AND TECHNOLOGY

UNIVERSITY OF NAIROBI

This thesis is submitted with our approval as research supervisors:

	Signature	Date
DR. JOHN O. ONYATTA DEPARTMENT OF CHEMISTRY UNIVERSITY OF NAIROBI John.onyatta@gmail.com		…09/06/2023……...
DR. PETERSON M. GUTO DEPARTMENT OF CHEMISTRY UNIVERSITY OF NAIROBI peterson.guto@uonbi.ac.ke	…………. ……	………09/06/2023.......
DR. IMMACULATE N. MICHIRA DEPARTMENT OF CHEMISTRY UNIVERSITY OF NAIROBI imichira@uonbi.ac.ke	…….. ………...	……12/06/2023………

DEDICATION

To my daughter, Pearl.

ACKNOWLEDGEMENT

ABSTRACT

Determination of phosphate levels in water is important in assessing the quality of drinking water and remediation of phosphate in water sources. Visible spectrophotometry is the standard technique that has been used for analysis of phosphates. However, this method is affected by interferences such as turbidity, salinity and high concentration of ions (silicate, arsenate and germanate). These interferences make analysis of phosphates at low concentrations difficult. The objective of this study was therefore to develop a voltammetry-based sensitive method for analysis of phosphates in water that would overcome interferences. Phosphate is not redox-active. Its electrochemical studies depend on its association with molybdate salts to form phosphomolybdate complex. Differential Normal Pulse Voltammetry (DNPV) and Cyclic Voltammetry (CV) were used to analyse the redox behaviour of the complex. Analysis by CV gave two redox centres with formal redox potentials of 0.167 ± 0.02 V and 0.357 ± 0.02 V with diffusion coefficients (D) of $1.408 \times 10^{-4}\ cm^2 s^{-1}$ and $5.629 \times 10^{-7}\ cm^2 s^{-1}$. Analysis of the complex using DNPV gave two responses, namely, 0.02 ± 0.001 V and 0.33 ± 0.001 V. The complex response varied with the concentration which made it possible to apply the technique for quantitative analysis of phosphates. Linearity of the method occurred between 0 – 8 mg/L of phosphate concentration, with a linear correlation coefficient of 0.9816. The limit of detection (LOD) and the limit of quantitation (LOQ) were found to be $0.06586\ mg/L$ and of $0.21952\ mg/L$ respectively. Accuracy was determined in terms of percent recovery and was found to range from 89 % to 102 %. Precision was also determined in terms of percentage relative standard deviation (percent RSD) of ten replicate measurements of a single concentration and the percent RSD was found to be 7.93 %. Both precision and accuracy were within acceptable limits for electrochemical methods of analysis. The developed method was then applied to natural water samples collected from lake Naivasha. Fifty water samples were collected in 50 ml plastic bottles and analysed using the developed method. The concentration of phosphates was found to be $0.6156 \pm 0.1046\ mg/L$ (at 95% confidence level), which was higher, compared to the previous studies. This could be attributed to the intensified human activities especially agricultural activities around the lake region over time. The study has shown that the method developed using DNPV could be more sensitive than CV. This is because it has a lower limit of detection, allowing it to be applied for the determination of low levels of phosphate. Further, the simplicity of the instrumentation is of significance in enhancing the possibility of sensor development for onsite use of the technique.

TABLE OF CONTENTS

LIST OF TABLES

LIST OF FIGURES

xi

LIST OF ABBREVIATIONS, ACRONYMS AND SYMBOLS

AE/CE,	Auxiliary Electrode / Counter Electrode
CV	Cyclic Voltammetry
DNVP	Differential Normal Pulse Voltammetry
DME	Dropping Mercury Electrode
LOD	Limit of Detection
LOQ	Limit of Quantitation
LCR	Linear Concentration Range
LSV	Linear Sweep Voltammetry
P	Phosphorus
RE	Reference Electrode
SWV	Square Wave Voltammetry
SHE	Standard Hydrogen Electrode
UV-Vis	Ultraviolet-Visible
WE	Working Electrode

CHAPTER ONE

INTRODUCTION

1.1: Background information

Phosphorus is an important element in biological systems and is mainly available to both animals and plants in form of phosphate. Phosphate is an important macronutrient in water which strongly influences microorganism growth (Schindler *et al.*, 2016). Over the past few decades, the amount of Phosphorus in the environment has increased, due to intensified agriculture and industrial activities. Large amounts of Phosphorus end up in water sources such as rivers and lakes, resulting in algal bloom, and hence eutrophication (Wurtsbaugh *et al.*, 2019).

The demand for phosphate in our daily lives has increased, resulting in increased environmental pollution, this is primarily due to the widespread use of fertilizers that contain high amounts of phosphates (Mogollón *et al.*, 2018). These phosphates ultimately end up in water sources, contributing to environmental pollution. During heavy rains, sewer wastewater especially in urban centres, rich in phosphates end up in water sources. The major problem of high amounts of phosphate in water is eutrophication. However, water for irrigation which has high phosphate level is recommended for crops, since phosphate is a nutrient which is central in the process of photosynthesis. Phosphate fertilizers are also applied to increase the amount of phosphates in soils for crops uptake (Guignard *et al.*, 2017).

Determination of phosphate is mainly through UV-Visible spectrophotometric techniques. These techniques are based on reaction of water with molybdenum salts to form a blue complex (phosphomolybdate) in acidic medium pH (0.5 - 2) which is then analysed by spectrophotometric technique to give the concentration of phosphate. However, this method suffers from matrix interferences since phosphate levels below 0.1mg/L cannot be determined accurately (Estefan *et al.*, 2013).

Electrochemical methods for analysis of heavy metals have been developed with great success, moreover electrochemical methods developed have been found to be inexpensive compared to spectrochemical methods (Wu *et al.*, 2019). So far electrochemical methods for trace analysis have been concerned with stripping voltammetry (Al-Hossainy *et al.*, 2017) and modified

surface electrodes, however, applying stripping voltammetry to non-metals requires modification of the working electrode (Amare, 2019). Voltammetric methods such as Linear Scan Voltammetry (LSV), Cyclic Voltammetry (CV), Differential Pulse Voltammetry (DPV) are popular for analysis of both organic and inorganic compounds (Zhu *et al.*, 2019). For any electrochemical method to be developed for non-metal analytes, the analytes must undergo reduction or oxidation reaction either in the presence of a reducing/oxidizing agent solution (homogeneous electron transfer) or at an electrode-solution interface (heterogeneous electron transfer) (Wang, 2004). However, many free occurring anions do not undergo redox reactions hence, these anions are detected in a combined form with another element whose oxidation state can change through electrolysis.

Therefore, the objective of this study was to develop a voltammetric method based on differential normal pulse voltammetry (DNPV) technique for determining phosphates in water. Such a method is expected to be sensitive with a low limit of detection compared to other methods.

1.2: Statement of the Problem

The standard method for analysis of phosphate in water is based on visible spectrophotometry. A reaction of a water sample with ammonium molydbdate forms phosphomolybdate complex (molybdenum blue complex) which is determined at a wavelength of 882 nm (Estefan *et al.*, 2013), however the standard method suffers from the following challenges:

Sample matrix: - samples with high turbidity especially saline samples from rivers, lakes, soils etc. result in light scattering which change the refractive index of light, leading to deviation from Beer-Lambert's law, and hence inaccurate results (Song *et al.*, 2016).

Bulky and expensive instrumentation: - Spectrophotometric method requires bulky and expensive instrument which are difficult to employ onsite (Song *et al.*, 2016).

To overcome the challenges posed by the standard method, different types of voltammetric methods for analysis of phosphates have been developed. Linear Sweep Voltammetric (LSV) method and Cyclic Voltammetry (CV) for analysis of phosphates in water have been developed and when compared to the standard method, LSV method had a lower limit of detection (Song

et al., 2016). Differential Pulse Voltammetry (DPV) and Square Wave Voltammetry (SWV) methods based on modified glassy carbon electrode were developed for determination of phosphate in biodiesel (Torrezani *et al.*, 2011).

A review by Osteryoung *et al.*, (1981) suggested that pulse techniques have a higher sensitivity i.e., almost 10 times higher than the conventional methods. Therefore, the development of a voltammetric method based on Differential Normal Pulse Voltammetry (DNPV) for determination of phosphate in water would be of significance in overcoming the interferences encountered during phosphate determination in water when using standard methods.

1.3: Objectives

1.3.1: General objective

The general objective of this study was to develop a highly sensitive differential normal pulse voltammetric method for determination of phosphates in waters.

1.3.2: Specific objectives

The specific objectives of this study were:

i.   To optimize the DNPV technique variables; amplitude, 1st and 2nd pulse widths, sampling widths, pulse period and quite time for the determination of phosphates.

ii.   To assess the redox behaviour of phosphomolybdate complex by DNPV technique.

iii.   To validate the proposed DNPV method in terms of Linear Concentration Range (LCR), Limit of Detection (LOD), Limit of Quantitation (LOQ), accuracy and precision for the determination of phosphates.

iv.   To evaluate the proposed DNPV method to determine phosphates in selected waters.

1.4: Justification and significance of the study

Phosphorus is an essential nutrient for both plants and animals. Phosphorus plays a critical role in photosynthesis in plants, in formation of bone and teeth in animals (Miedlich *et al.*, 2010), it also serves as a building block for the cell membrane in small microorganisms like phytoplankton (Martin *et al.*, 2011). The acquisition of Phosphorus by both plants and animals mainly occurs through water, with phosphate being the primary biologically available chemical species of Phosphorus.

However, the increased levels of phosphate in water resulting from intensified agriculture, industrial activities, and point release of treated wastewater into the environment pose a significant environmental challenge (Sharpley *et al.*, 2015). The high levels of phosphate in water bodies have been linked to eutrophication in fresh water lakes and estuarine environments since the 1970s. This issue highlights the pressing need for monitoring and determining the levels of phosphate in water to mitigate the negative impacts of eutrophication on aquatic ecosystems (Jarvie *et al.*, 2013).

This study aims to provide an accurate and sensitive method for the determination of low levels of phosphate in water using DNPV, which offers improved sensitivity compared to the standard method. The study's significance lies in its potential to provide a valuable tool for effective monitoring and management of water quality by enabling reliable determination of phosphate levels in water samples.

CHAPTER TWO

LITERATURE REVIEW

2.1: Phosphorus in the environment

Phosphorus is a vital nutrient element that is utilised by both plants and animals for energy transport, growth and development (Hodges, 2010). The terrestrial environment is the largest reservoir of Phosphorus with $8 - 40 \times 10^{17} \ Kg$ n sediments, $9.6 - 20 \times 10^{14} \ Kg$ in soils at a depth of less that 60 meters. The major Phosphorus reservoir in the aquatic environment is the ocean with $2700 \times 10^9 \ Kg$ at a depth of 300 meters from the surface. The atmospheric environment has the least amount of Phosphorus i.e. $3.0 \times 10^7 Kg$ (Worsfold *et al.*, 2016). The major Phosphorus exchanges occur between the marine bio-systems and the soil biota and ocean water, and from soils into the ocean. Weathering of rocks, erosion of soils and transport of particulates also contribute to Phosphorus exchanges in the environment. A schematic diagram of Phosphorus cycle is shown in Figure 2.1.
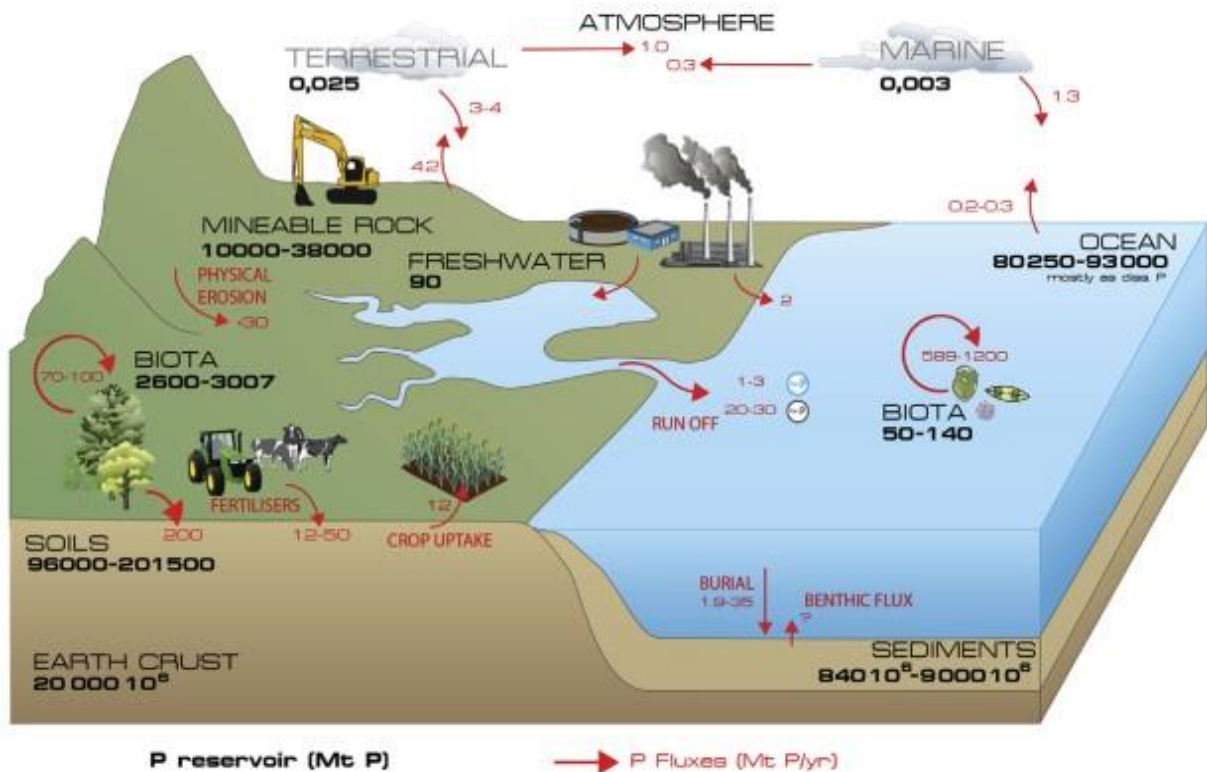
Figure 0.1: A schematic diagram of Phosphorus cycle, showing Phosphorus fluxes in terrestrial, atmospheric and marine environment (Worsfold, *et al.,* 2016).

Increase in agricultural activities has raised the demand for Phosphorus which has led to significant impacts on water quality. The agricultural runoffs during heavy rains containing phosphates from fertilizers are transported to water bodies resulting in elevated levels of Phosphorus. This has consequently led to eutrophication, algal blooms, oxygen depletion in water and consequently death of biota (Withers *et al.*, 2014). Increased industrialization, population growth especially in urban areas have increased Phosphorus input to natural waters for example through release of sewage treatment (Bowes *et al.*, 2009).

2.1.1: Forms of Phosphorus in the environment

There are various species of Phosphorus present in the environment. Dissolved inorganic phosphates, these are inorganic orthophosphates and polyphosphates. Phosphorus in the form of orthosphosphates is the major form of Phosphorus that is biologically available. Dissolved organic phosphates are proteins, nucleic acids, phosphoamides, amino phosphonates, phospholipids, sugar phosphates and organic Phosphorus. Particulate Phosphorus, includes clay and silt-associated inorganic and organic Phosphorus (Worsfold *et al.*, 2016). Phosphorus is present in various forms in natural waters which provides a challenge in developing analytical methods that are reliable, sensitive and accurate for determination of concentration of individual Phosphorus species. The various forms of Phosphorus in natural waters are shown in Figure 2.2.
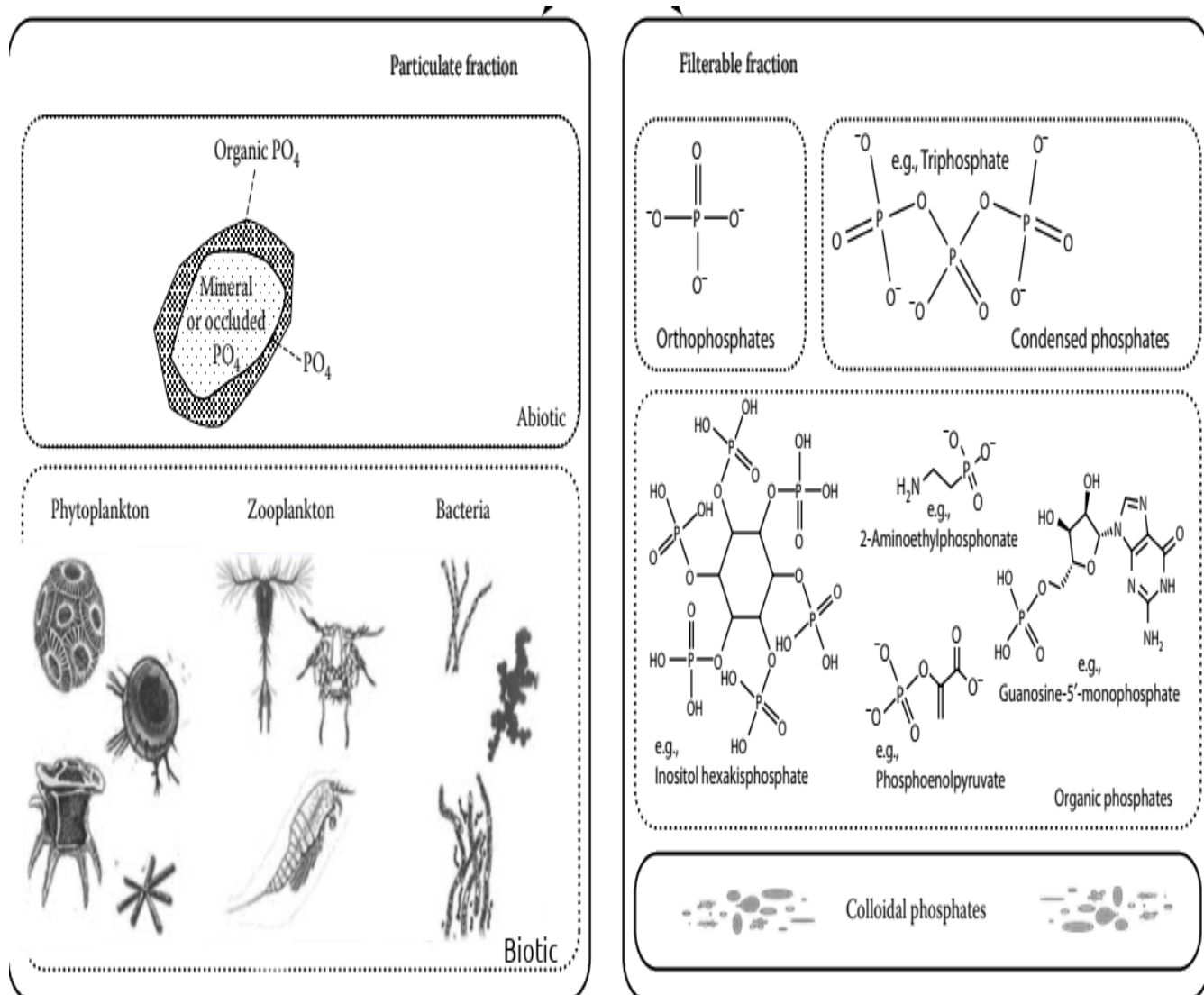
Figure 0.2: Forms of Phosphorus in natural waters, (Estefan, *et al*., 2013).

2.1.2: Forms of Phosphorus in natural waters

Phosphorus present in water can broadly be classified into particulate and filterable Phosphorus. Determination of various fractions of Phosphorus is usually done through a sequence of steps which require sample preparation followed by determination of various fractions of Phosphorus as shown in Figure 2.3.
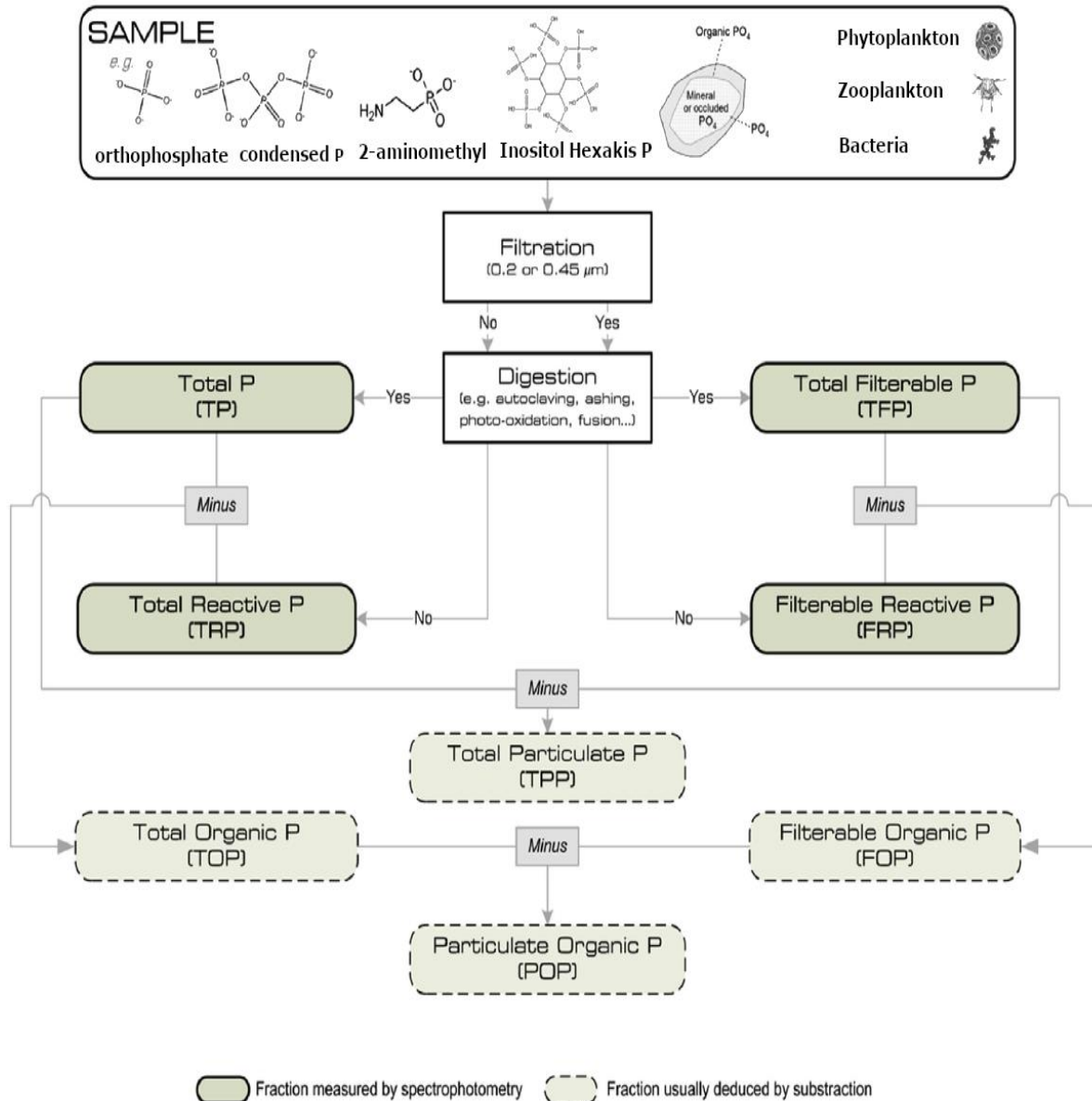
Figure 0.3: Determination of different fractions of Phosphorus (Worsfold *et al.,* 2016)

Phosphorus availability as a nutrient in many aquatic environments is reliant on processes that promote the release of Phosphorus from phosphate rocks (Hartmann *et al.*, 2014). Rock weathering and erosion processes releases Phosphorus either in particulate or dissolved forms into marine environments and these processes act as the limiting factor in primary production of phosphate (Benitez-Nelson, 2000). In recent decades the impact of Phosphorus on water quality due to agricultural activities have received research attention due to effects of Phosphorus on downstream environments, that is marine and estuarine environments (Macdonald *et al.*, 2016). Macdonald *et al* (2016) proposed a framework of integrating crucial ecosystem function and processes, whose main objective was to control Phosphorus fluxes

from terrestrial to aquatic environment which in turn would moderate Phosphorus releases due to human activities mainly agriculture and wastewater.

Schindler, (1971) established that Nitrogen and Phosphorus as the limiting nutrients of primary producers in aquatic and terrestrial ecosystems. Fertilizers are applied to increase the amount of Nitrogen and Phosphorus in order to improve crop yields (Guignard *et al.*, 2017). However, excessive Phosphorus and Nitrogen inputs have greater ecological and long-term impacts from individual species to the whole ecosystem. Phosphorus and nitrogen are essential for the process of photosynthesis, promoting growth of cells, metabolism and synthesis of proteins (Chapin *et al.*, 2011).

2.2:   Effects of excess phosphate in water

Excessive enrichment and transformation of lake ecosystems commonly known as eutrophication is a problem that was identified and studied in 1970 by David W. Schindler (Schindler, 1971). Schindler (1971) demonstrated that phosphate was the primary limiting nutrient, which was responsible for eutrophication. Through a series of experiments, he showed that a combination of phosphate (PO_4^{3-}) and nitrate (NO_3^-) caused large algal blooms in lakes, however a slight response to PO_4^{3-} was detected but no response was observed when (NO_3^-) was tested for eutrophication. Schindler, (1971) concluded that Phosphorus was solely responsible for eutrophication. According to Schindler *et al.*, (2016) lake eutrophication could be reduced by reduction of Phosphorus. Due to increase in industrialization, population and agricultural practices, monitoring of phosphates in water is of concern (Withers *et al.*, 2014).

2.3:   Techniques for determination of phosphates

Several analytical techniques which include, spectrophotometry, separation, automated and electrochemical techniques have been used for determination of phosphates (Estefan *et al.*, 2013). Spectrophotometric technique is based on detection of vanadomolybdophosphoric complex (yellow in colour) acid or phosphomolybdenum blue complex/phosphomolybdate complex (blue in colour). Separation techniques such as ion chromatography has been used in analysis of different species of Phosphorus that is, orthophosphates, condensed phosphates and organic phosphates in analysis of phosphates in wastewaters (Urasa and Ferede, 1986). Other separation based methods for determination of phosphates in water include, High Performance Liquid Chromatography, Capillary Electrophoresis and Liquid Waveguide Capillary Cell

(Neves *et al.*, 2008). For analysis of many samples, automated techniques are mostly favoured. Examples of automated techniques that are widely used are, Segmented Continuous Flow Analysis (SCFA), Sequential Injection Analysis (SIA) and Flow Injection Analysis (FIA) (Patey *et al.*, 2008). Determination of phosphates is mainly through optical techniques or electrochemical techniques (Estela and Cerdà, 2005).

2.3.1:   Ultraviolet-visible molecular absorption spectrometry

Molecular Absorption Spectroscopy is mostly employed in qualitative/quantitative analysis of both organic and inorganic molecules (Penner, 2017). The absorption of radiation by inorganic species can be explained by considering the elements in the first two transition series that form complexes with other compounds. These complexes absorb wavelengths of visible radiation in one or several oxidation states to form coloured compounds. Absorption occurs when there is transition of electron(s) between filled and unfilled d-orbitals having energy that is dependent on the molecules (ligands) bonded to the metal ion (often centrally located) (Skoog *et al.*, 2013).

2.3.2:   Molecular absorption spectrophotometry

In molecular absorption spectrophotometry, an analyte absorbs electromagnetic radiation in the wavelength range of $190nm$ to $800nm$ (Skoog *et al.*, 2017). The concentration of the analyte is determined by measurement of transmittance T or the absorbance A of a solution contained in a transparent cell of length l. The concentration of the analyte relates to absorbance according to Beer-Lambert law (Equation 2.1).

Beer-Lambert law states that the absorbance of light by a solution is directly proportional to the concentration of the absorbing species in the solution and the path length of the light through the solution (Skoog *et al.*, 2017). Mathematically, it is expressed as,

$$A = -\log T = \log \frac{P_o}{P} = \varepsilon bc \qquad (2.1)$$

Where P_o is the incident radiant power, P is the transmitted radiant power, A is the absorbance, T is the transmittance, b is the path length of sample, c is the concentration of analyte and ε is the molar absorptivity (Figure 2.4)
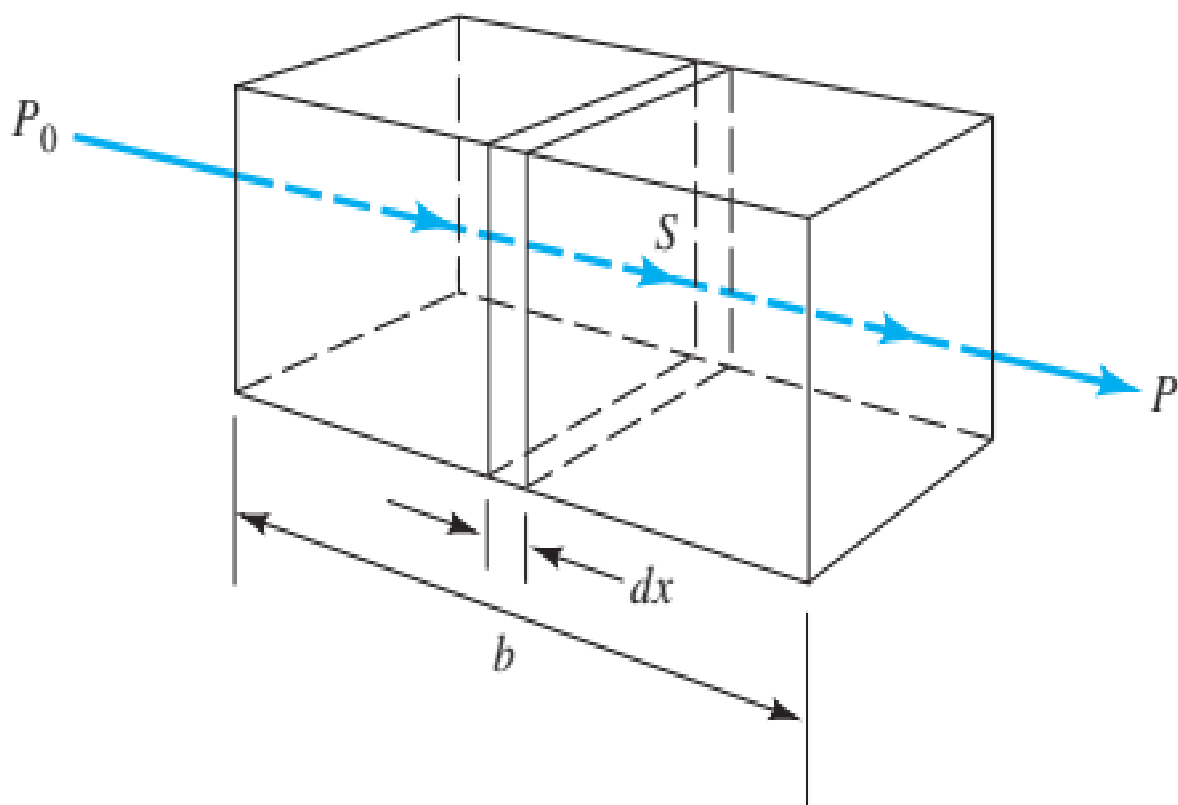
Figure 0.4: Attenuation of initial radiant power Po to transmitted power P by an absorbing solution containing c moles per litre with a pathlength b (Skoog *et al.*, 2017).

By applying Beer-Lambert law, the concentration of a solution to be calculated by measuring its absorbance. During quantitative analysis, it cannot be assumed that Beer-Lambert law will apply i.e. that the relationship between absorbance and concentration is linear (Christian *et al.*, 2014). Deviations from the law occurs due to real, chemical and instrumental factors. Real deviations are due to fundamental limitation of the law. They are mainly caused by high concentration (usually > 0.01M) that affects analyte environment and absorptivity. Instrumental deviations are a result of how absorbance measurements are made. Beer-Lambert's law applies only with a monochromatic light source; however, polychromatic light sources are mostly used, this poses a challenge of selecting a narrow wavelength from the light source. Chemical deviations are changes in concentration especially when an analyte reacts with a solvent to produce a product with altered absorption characteristics (Skoog *et al.*, 2017).

2.3.2.1: Ultraviolet-visible spectrophotometers

The various types of UV-Vis spectrophotometers are, Single beam, double beam in space, double beam in time and multichannel spectrophotometers. Modern spectrophotometers are based on a double beam design. Single beam instruments are designed to measure absorbance as a function of time (Harris, 2010). Figure 2.5 shows single beam and double beam spectrophotometer designs.
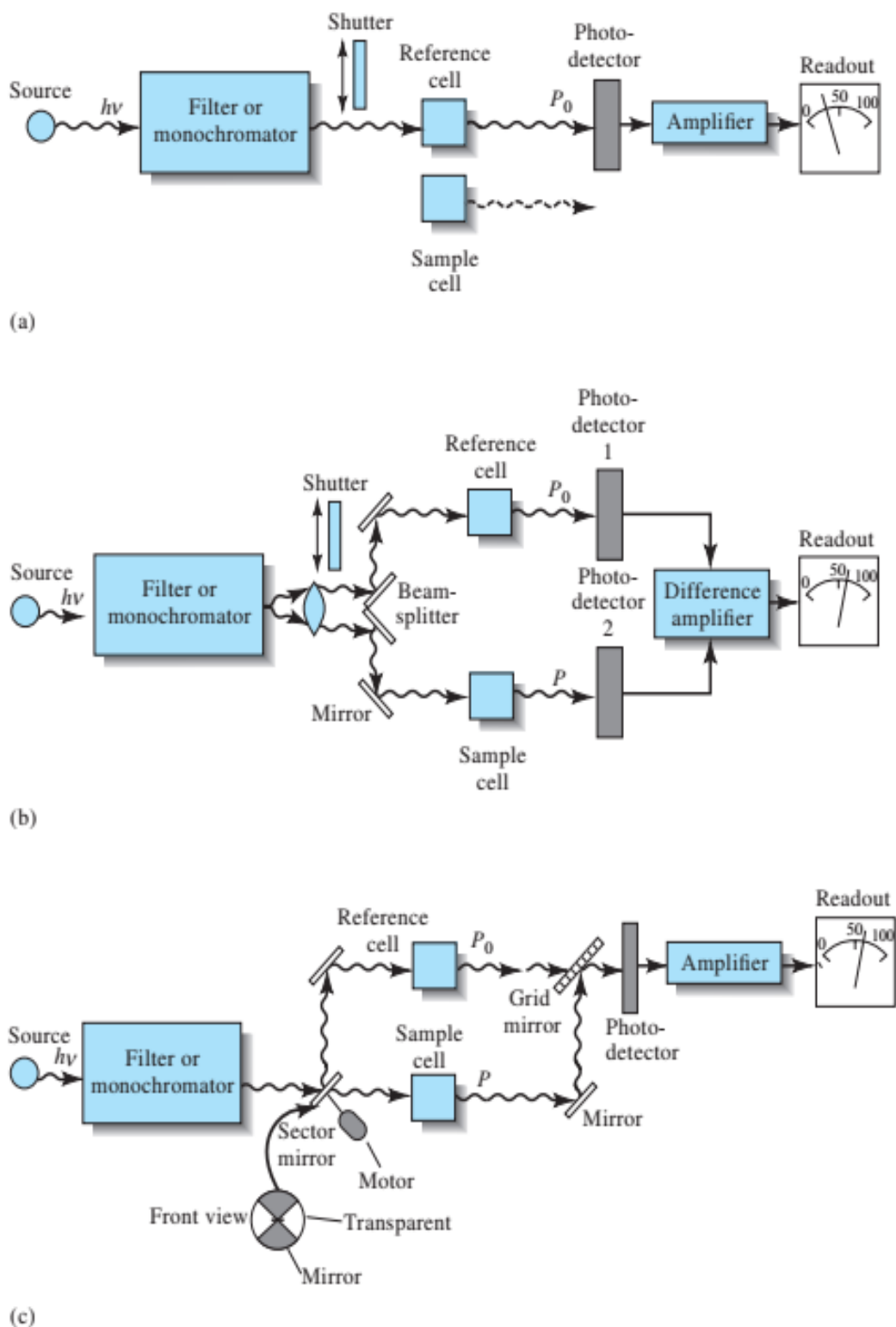
Figure 0.5: Instrumental design for UV-Vis spectrophotometers (a) Single Beam spectrophotometer (b) Double Beam in space spectrophotometer (c) Double Beam in time spectrophotometer (Skoog *et al.*, 2017).

A UV-Vis Spectrometer have five major parts (Figure 2.6). The parts are, (1) *Light source*: This is the source of continuous radiation over a wide range of interest. (2) *Monochromator:* It disperses light into a narrow band of wavelength. (3) *Sample cell/cuvette:* It's a transparent container that holds the sample. (4) *Detector:* It's a device/transducer that converts radiant power to electrical signal. (5) *Read out:* A device that displays the response of the detector in a human readable form (Christian *et al.*, 2014).
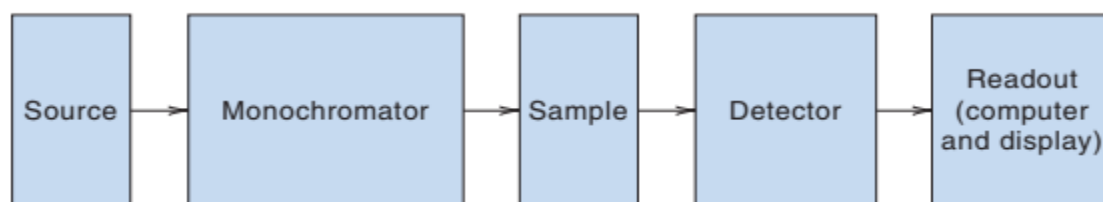
Figure 0.6: Block diagram of a spectrometer (Christian *et al.*, 2014)

2.3.2.2: Quantitative analysis and calibration graphs

Many inorganic and organic molecules have strong absorption bands in UV-Vis region of electromagnetic spectrum. However, if the absorption of UV-Vis radiation by an analyte is poor, it is often reacted with another species to form a product that absorbs strongly (Harvey, 2011).

In order to determine an analyte concentration by instrumental technique, a standard calibration graph is usually needed. A series of standards, samples of known concentration usually six or more are measured using an analytical instrument. The results are then used to plot a calibration graph of signals (measurements from the analytical instrument) against standard concentrations as shown in Figure 2.7. Concentration of an unknown sample is then determined by interpolation. In UV-Vis spectrometry the signal is a measure of absorbance of the analyte (Miller and Miller, 2010).
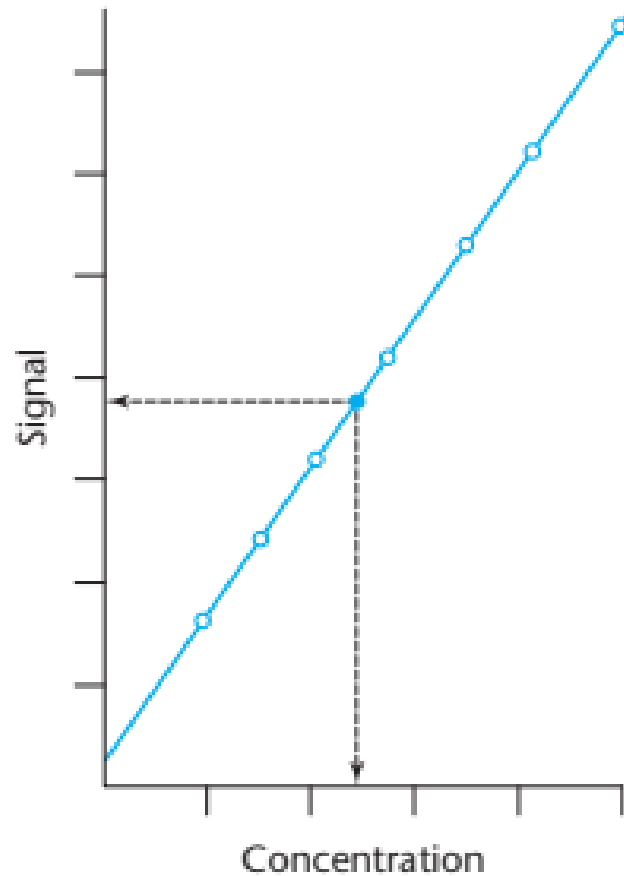
Figure 0.7: Standard Calibration Graph (Miller and Miller, 2010).

2.3.2.3: Analysis of phosphates by spectrophotometric technique

The standard method for analysis of phosphates is based on visible spectrophotometry. This method is based on the reaction of orthophosphate (PO_4) with ammonium heptamolydbdate ($(NH_4)_6Mo_7O_{24}$) to form phosphomolybdic acid ($H_3PMo_{12}O_{40}$). The complex formed is then reduced by ascorbic acid ($C_6H_8O_6$) in presence of potassium antimony tartrate to form molybdenum blue. Another method for analysis of phosphates involves a reaction of orthophosphates with ammonium salt to form phosphomolybdic acid which in the presence vanadium, forms a yellow vanadophosphomolydic acid. In both methods the intensity of the colours is a measure of the concentration of phosphate, however a yellow, vanadophosphomolydic does not produce an intense colour for measurement (Pradyot, 2018) especially if the sample is turbid. Hence, the method in which molybdate blue is formed, is usually preferred (Song *et al.*, 2016).

In molybdenum blue method, the concentration of phosphate is measured at a wavelength of 882 nm while that of vanadophosphomolydic acid is determined at 470 nm. The sensitivity of vanadophosphomolydic method is less compared to that of molybdenum blue method however, it suffers less from interfering ions (Estefan *et al.*, 2013). Due to its high sensitivity, molybdenum blue method is the standard method for analysis of phosphates in water (Keneth, 1990). The reactions involved in the formation of phosphomolybdic acid and molybdenum blue are shown in Equations 2.2 and 2.3.

$$72H^+ + 7PO_4^{3-} + 12Mo_7O_{24}^{6-} \rightarrow 7PMo_{12}O_{40}^{3-} + 36H_2O \qquad (2.2)$$

$$PMo_{12}O_{40}^{3-} + 2C_6H_8O_6 \rightarrow PMo_{12}O_{40}^{7-} + 2C_6H_6O_6 + 4H^+ \qquad (2.3)$$
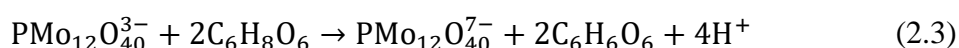
Both methods involve reaction of $PMo_{12}O_{40}^{3-}$ ion known as Keggin anion (Son *et al.*, 2013) with different reducing agents for example ascorbic acid ($C_6H_6O_6$) is the mostly used reducing agent.

2.3.3: Electrochemical techniques for phosphate determination.

The use of electrochemical instruments has increased due to the need for simple, rapid, inexpensive and portability of the instruments. These methods have been developed for metals, organic and inorganic compounds. Due to their portability, the demand for electrochemical methods that can be used by non-experts is high. Methods based on potentiometry and voltammetry for the determination of phosphates continue to be developed (Villalba *et al.*, 2009).

2.3.3.1: Potentiometric methods

The earliest determination of phosphate ions by an electrochemical approach was based on potentiometry (Campanella *et al.*, 1983) where lead (Pb) was used an Ion Selective Electrode (ISE). Compared to the standard method, this approach had several advantages, including its speed, simplicity, and the fact that it doesn't require complex sample preparation procedures. ISE methods provide an excellent analytical method for investigation of trace metals in environmental waters (Radu and Diamond, 2007). However, Ion Selective Electrode (ISE) methods lack selectivity and sensitivity in quantitation of trace analytes in presence of complex sample matrices such as sea waters, lakes and rivers (De Marco *et al.*, 2007).

Potentiometric methods for analysis of phosphates require concentration of phosphate to change as the sample is being added. Selectivity for these methods is a major concern because related ions also affect the potential and hence interfere with the measurement of the analytical signal of interest. To overcome this challenge (Glazier and Arnold, 1988) attempted to develop phosphate selective membranes but it proved difficult to design such a polymer membrane because of the size and the hydrophilic nature of phosphate molecule (Villalba *et al.*, 2009).

2.3.3.2: Voltammetric methods

Orthophosphate (PO_4^{3-}) is not directly available for voltammetric analysis. Voltammetric analysis which involve PO_4^{3-} ions, depend on their association with molybdate complexes. The procedure for formation of phosphomolybdate blue complex has been described under spectrophotometric technique (*Section 2.3.2.3.*). There are several types of voltammetry-based methods that have been developed for determination of PO_4^{3-} by (Fogg and Bsebsu, 1981) and (Fogg *et al.*, 1981).

In voltammetry a current is measured as a function of applied potential. The current measured is usually related to the concentration of an electroactive analyte. This process is normally accomplished by monitoring electron transfer during a redox process of an analyte as demonstrated by Equation 2.4.

$$O + ne^- \rightleftharpoons R \qquad (2.4)$$
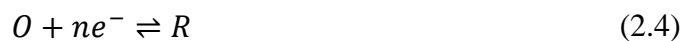
Where O and R are the oxidized and reduced forms of the redox reaction. For systems that obey laws of thermodynamics, electrode potential can be used to measure the concentration of the electroactive analyte at the electrode surface $[C_O(0, \ t)]$ and $[C_R(0, \ t)]$ according to the Nernst equation, i.e., Equation 2.5 below.

$$E = E^o + \frac{2.3RT}{nF} \log \frac{C_O(0, \ t)}{C_R(0, \ t)} \qquad (2.5)$$

Where E^o is the standard potential for the redox reaction, R is the universal gas constant $(8.314 JK^{-1}mol^{-1})$, T is temperature in Kelvin, n is the number of electrons transferred in the reaction and F is the Faraday's constant $(96,487 \ Coulombs)$. If E^o is negative, the forward reaction is more favourable and the oxidized species is reduced. The current responsible for change in oxidation state is known as the Faradaic current (Wang, 2000).

In voltammetry, the relationship between applied potential and Faradaic current in which the rate of redox reaction is measured by Faradaic current. A plot of current i, against applied potential E is known as a voltammogram. Equation 2.6 shows the relationship between applied potential and diffusion current.

$$E = E_{\frac{1}{2}} + \frac{RT}{nF} \ln \left(\frac{i - i_d}{i} \right) \tag{2.6}$$

Where $E_{1/2}$ is the potential at which the value of the current is half of the peak commonly known as half-wave potential, i is the measured current and i_d, is the diffusion current. Cottrell equation describes the diffusion current as expressed in Equation 2.7.

$$i_d = nFAC_0 \left(\frac{D}{\pi t} \right)^{\frac{1}{2}} \tag{2.7}$$

Where A is the area of the planar electrode in cm^2, D is the diffusion coefficient for c_o species, and t is time in seconds.

Non-Pulse Voltammetric Techniques

Linear Scan Voltammetry (LSV) and Cyclic Voltammetry (CV) techniques have been used for analysis of PO_4^{3-} in water. In order to determine PO_4^{3-} in fresh water and to minimise silicate interferences Song *et al.*, (2016) analysed phosphomolybdate complex by LSV and reported that the deviation of LSV method and spectrophotometry method was less than 10%. They obtained better results when they used LSV technique to analyse water samples collected from a pond, rivers and lakes compared to spectrophotometric method.

Pulse Voltammetric Techniques

Pulse techniques were used to analyse phosphates as early as 1981. Fogg *et al.,* (1981) determined phosphate on a glassy carbon electrode. This method was based on Differential Pulse Voltammetry (DPV). They were able to determine the concentration of both silicate and phosphate at 10^{-7} and 10^{-6} M levels respectively. Arsenate could only be determined at $10^{-5} M$ however, in the determination of germanate, there was an interference due to its adsorption at the glassy carbon electrode. The study showed that silicate, arsenate and germanate interreferences could be discriminated by DPV technique. This study demonstrated that glassy carbon electrode is sensitive in the determination of phosphates.

Differential Normal Pulse Voltammetry (DNPV)

Pulse voltammetric techniques are a family of electrochemical methods that use a train of potential pulses to obtain a corresponding current response in order to generate current-potential voltammograms. Pulse voltammetry exploits the difference between faradaic and non-faradaic processes so as to discriminate against the background, in order to improve signal to noise ratio (S/N). Compared to LSV and CV (continuous electrolysis) pulse voltammetry techniques are more sensitive (have higher S/N ratio) (Fogg *et al.*, 1981).

The use of potential pulses and measuring current at the end of the pulse was proposed in 1958 (Barker, 1958), however the application of this technique became popular in 1970s after the advent of electronic devices and computers. The first pulse voltammetry experiment was done using a Dropping Mercury Electrode (DME), a technique known as pulse polarography (Stojek, 2010). The latest advancements in pulse voltammetry techniques are not constrained to the use of DME alone. Other electrode materials like glassy carbon, platinum, and gold electrodes have also been employed. (Molina *et al.*, 2001).

Aoki *et al.*,(1980), Lovrić and Osteryoung, (1982) established the theory of DNPV in which DNPV was considered as a modified form of Differential Pulse Voltammetry (DPV). It involved a method in which two potential steps with similar short durations were superimposed on the rest potential. Short double potential pulses of duration t_1 and $t_2 - t_1$ and amplitude $E_1 - E_o$ and $E_2 - E_o$ respectively were superimposed on the rest potential E_o at which no faradaic current flowed as shown in Figure 2.8 and Figure 2.9.
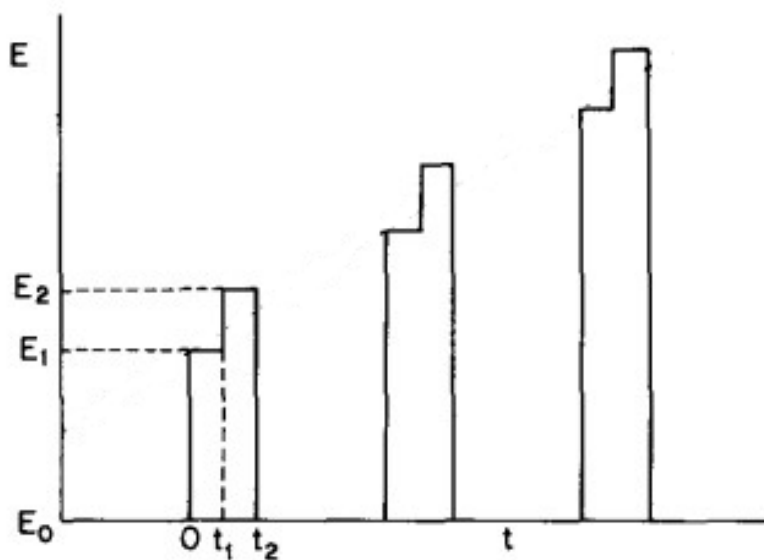
Figure 0.8: Potential time function for DNPV (Aoki *et al.*, 1980)
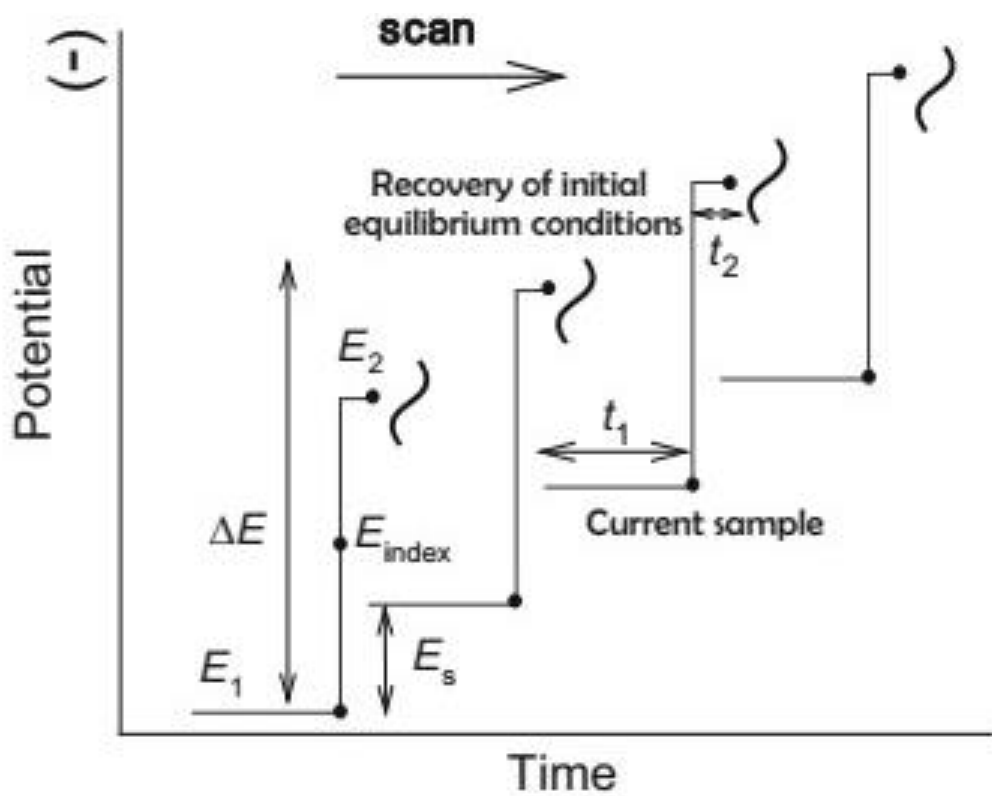
Figure 0.9: Potential-time programme (Molina, 2016)
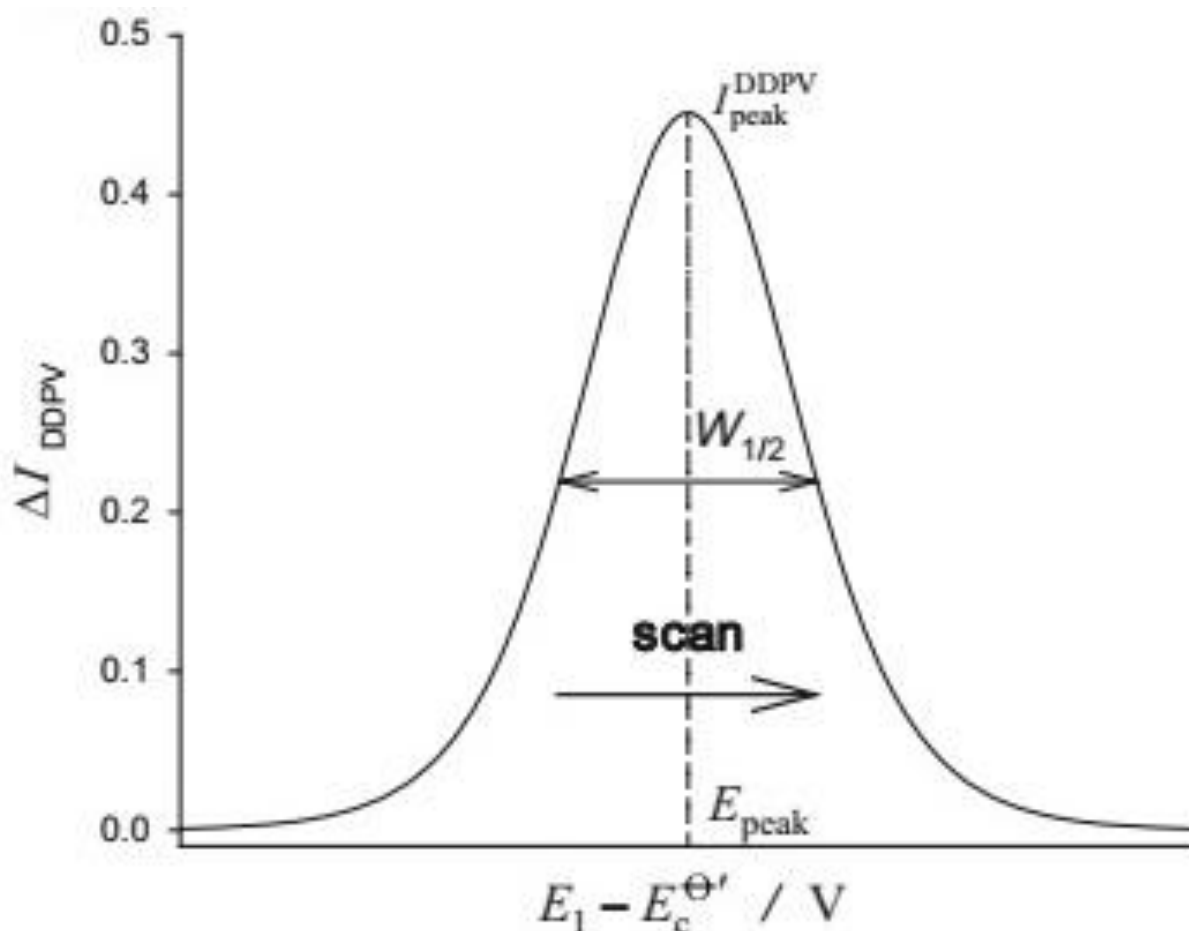
Figure 0.10: DNPV/DDPV Response, a plot of ΔI against E-E⁰ (Molina, 2016) Note E⁰=E$_{1/2}$

The time duration between pulses $(t_2 - t_1)$ at potential E_o is made large so that it is not a parameter of the experiment. Current is measured at the end of each pulse i.e., at t_1 and t_2. The current i, potential E, curve is a plot of the difference $\Delta i = i(t_1) - i(t_2)$ as a function of potential E_1 (Aoki *et al.*, 1980) or versus an average potential $E_{1,2} = (E_1 + E_2)/2$. (Molina and González, 2016). This technique may be viewed as a combination of normal and differential pulse wave-forms. It is important to note that the difference $\Delta E = E_2 - E_1$ is kept constant and the two potential pulses have similar duration during the experiment. After the decay of the pulse, the initial equilibrium position is recovered (Figure 2.9). This technique is also known as Differential Normal Double Pulse Voltammetry DNDPV/DDPV since double pulses are used. Figures 2.8 and 2.9 show potential time program and a DDPV response, courtesy of Molina and Gonzalez (2016).

According Osteryoung *et al.*, (1981) and Carter, (2000), Differential Pulse Voltammetric (DPV) methods offer the following advantages over non-pulse techniques (e.g., LSV and CV)

21

(1) Current-Potential curves similar to direct current polarographic waves are obtained. (2) Residual Resistor-Capacitor (RC) currents due to charged Helmholtz double layer are minimized or nearly eliminated. (3) High sensitivity of current response since measurements are made at short durations. At two successive potential pulses, Double Pulse Differential Voltammetry techniques combine faradaic currents hence recovering the initial equilibrium conditions, this offer a distinct advantage of high sensitivity due to, minimization of background current and double layer (Molina and González, 2016).

Double potential pulse techniques in recent years have been employed for study of reaction mechanisms and kinetics. These studies have become important especially for microelectrodes, leading to theoretical and experimental development of these techniques. The combination of pulse techniques and microelectrodes offers important advantages in terms of accuracy due to reduction in charge current and ohmic drop. This provides well defined signals that are excellent for electrochemical studies (Batchelor-McAuley *et al.*, 2015). The subtractive nature of the DDPV methods makes them suitable for quantitative analysis as the background current is reduced and peak shaped signals are obtained (Molina *et al.*, 2001).

The theoretical equation for $(\Delta I - E_1)$, Differential Pulse Polarographic curves for reversible process were first derived by Parry and Osteryoung, (1965). The derived equations are presented as follows.

The polarographic current-potential given in Equation 2.6 (*section 2.3.3.2*), is rearranged for i to yield Equation 2.8.

$$i = i_d \left[\frac{1}{1 + \exp\left(E - E_{\frac{1}{2}}\right) \frac{nF}{RT}} \right] \tag{2.8}$$

Where i is the measured current, and i_d is the diffusion current. When Equation 2.8 is differentiated and Cottrell Equation 2.7 (*section 2.3.3.2*) substituted, Equation 2.9 is obtained (Bard and Fulkner, 2000).

$$\Delta i = \frac{n^2 F^2}{RT} AC \Delta E \sqrt{\frac{D}{\pi t}} \frac{P}{(1+P)^2} \tag{2.9}$$

Where $P = \exp\left(E - E_{\frac{1}{2}}\right) nF/RT$. Equation 2.8 is only valid for small values of pulse amplitudes. Maximizing Δi with respect to E by differentiating Equation 2.8 and equating to zero, P is found. $P = 1$ when Δi is maximum, thus the maximum current Δi_{max} is given by Equation 2.10.

$$\Delta i_{max} = \frac{n^2 F^2}{4RT} \, AC \, \Delta E \sqrt{\frac{D}{\pi t}} \tag{2.10}$$

However, for practical purposes it is of interest to find the relation of Δi_{max} for a large pulse. From Equation 2.9 we obtain a difference in current by subtracting i at E_1 from i at E_2, this yields Equation 2.11.

$$\Delta i = i_d \left[\frac{P_A \sigma^2 - P_A}{\sigma + P_A \sigma^2 + P_A + P_A^2 \sigma}\right] \tag{2.11}$$

Where $P_A = \exp(\frac{E_1 + E_2}{2} - E_{1/2})\frac{nF}{RT}$ and $\sigma = \exp(\frac{E_2 - E_1}{2})\frac{nF}{RT}$ and $E_2 - E_1 = \Delta E$, the pulse amplitude. By substituting the Cottrell equation (Equation 2.7) for i_d we find Equation 2.12.

$$\Delta i = nFAC \sqrt{\frac{D}{\pi t}} \left[\frac{P_A \sigma^2 - P_A}{\sigma + P_A \sigma^2 + P_A + P_A^2 \sigma}\right] \tag{2.12}$$

P_A is 1 when Δi is maximum, therefore the expression for the maximum current becomes.

$$\Delta i_{max} = nFAC \sqrt{\frac{D}{\pi t}} \left(\frac{\sigma - 1}{\sigma + 1}\right) \tag{2.13}$$

For Differential Normal Double Pulse Voltammetry (DNDPV) (Molina and González, 2016) deduced from Equation (2.13) the expression of current ΔI at both very positive and negative potential that is valid for any geometry of the electrode (spherical, disc, etc.) given by Equation 2.14.

$$\Delta I = FADC_O^* \left(f(\tau_1 + \tau_2) - f(\tau_1)\right) \tag{2.14}$$

Where $f(\tau_1 + \tau_2)$ is E_2 expressed as a function of time $\tau_1 + \tau_2$ and $f(\tau_1)$ is E_1

$$\frac{\Delta I}{FADC_o^*} = \frac{1}{\sqrt{\pi D}} \left(\frac{1}{\sqrt{\tau_1 + \tau_2}} - \frac{1}{\sqrt{\tau_1}}\right) \tag{2.15}$$

Molina and González, (2016) noted that as τ_2 increases, DNDPV curves calculated from disc, spherical and planar electrodes, result in a decrease in peak current (Equation 2.13).
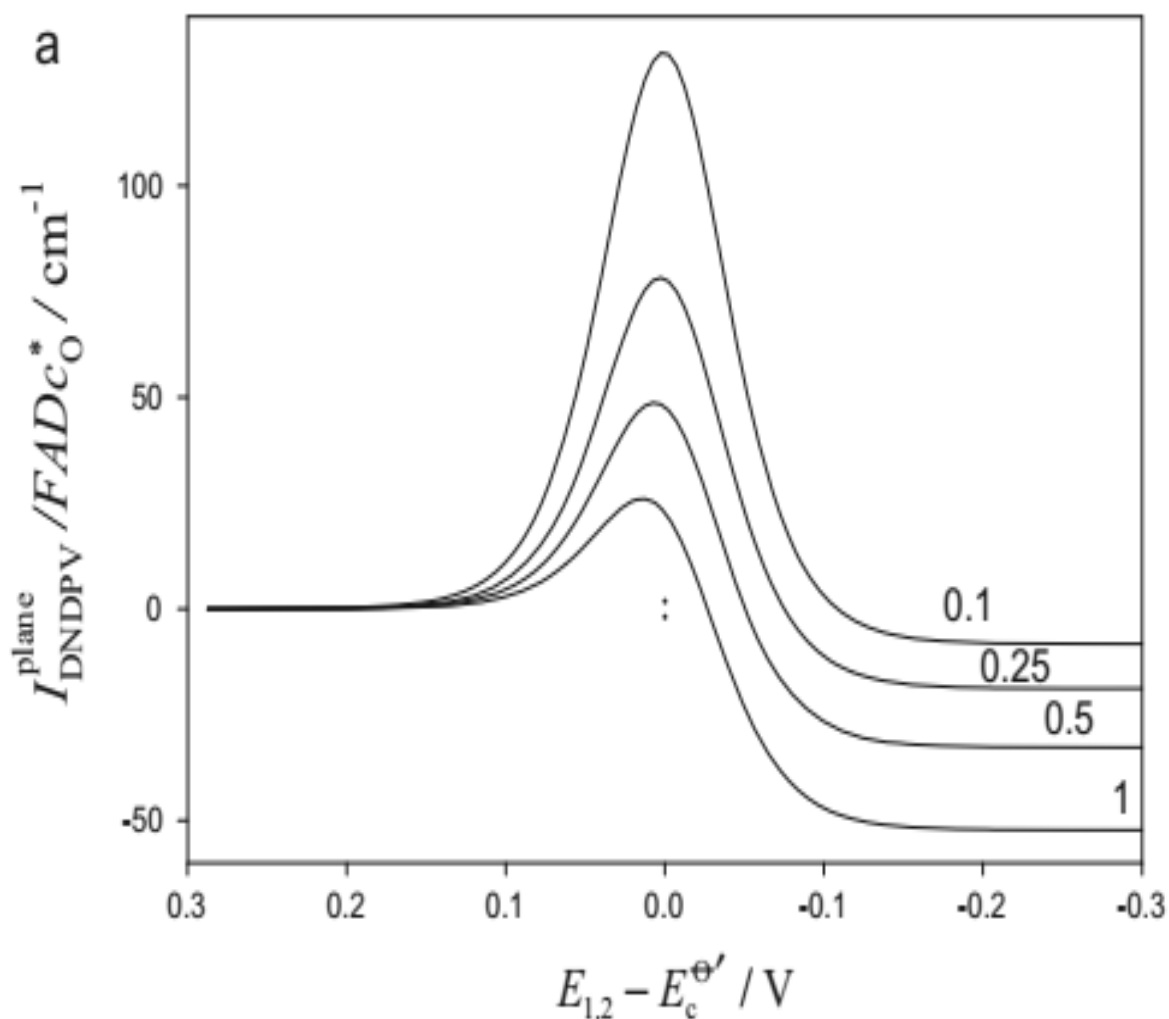
Figure 0.11: Influences on DNDPV curves calculated from a planar electrode diameter, $R_d=$ 25 μm, Diffusion Coefficient D = 10^{-5} cm^2 s^{-1}, pulse period $\tau = 1$ s. The values of τ (0.1, 0.25, 0.5 and 1) in seconds are shown on the curves (Molina and González, 2016).

It is however important to note that the pulse width of the two pulses in DNPV is the same i.e., $\tau_2 - \tau_1 = \tau_1$. There are other derivations of DNPV which yield similar results. These theories are based on the theory of complex convolution of Laplace transformations (Aoki *et al.*, 1980).

2.3.3.3: Electrochemical cell

Voltammetric methods involve the application of a potential from an external source to an electrode known as a Working Electrode (WE) and measurement of current that flows as a result of the applied potential at the Auxiliary Electrode (AE). In order to control the applied

potential, a potentiostat is used. A potentiostat electronically separates the Reference Electrode to ensure that no current flows through it, while allowing the current to flow through the WE and the AE. Modern potentiostats are constructed using electronic devices such as operational amplifiers, they include waveform generators that allow application of time dependent potential such as a train of potential pulses to the WE. (Elgrishi *et al.*, 2018).
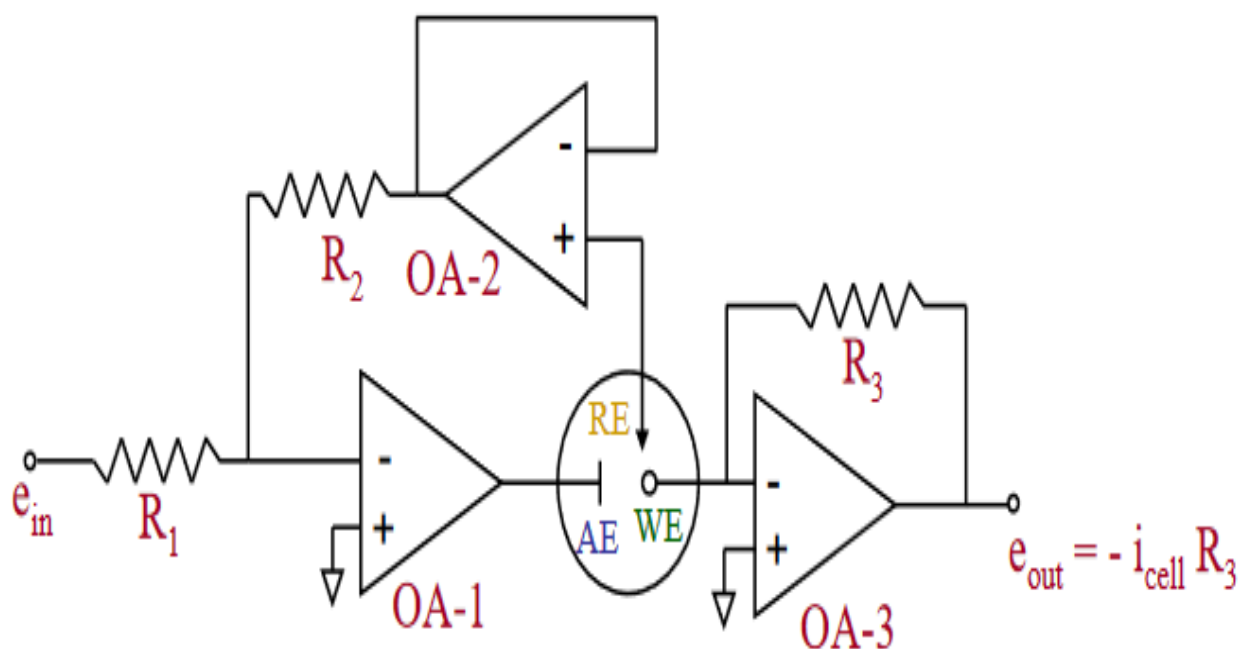
Figure 0.12: A basic Potentiostat constructed from 3 Operational Amplifiers (OA) and Resistors (Dryden and Wheeler, 2015).

In order to minimise the resistance of the solution between the electrodes, the tips of the electrode are kept close together. The three electrodes can be placed together in the same solution, however, in some circumstances AE or RE may be physically isolated from WE in contact with the solution, for example leakage of RE component such as Ag^+ into the solution may result in undesirable reactions. In modern cells this problem is solved by using a membrane of glass frit which separates compartments of the electrochemical cell. Other consideration is removal of oxygen from the cell, which is done by sparging the solution with nitrogen for about 5 minutes, (it is usually common to have a sparge tube) in an electrochemical cell (Harvey, 2011). The electrochemical cell and the three-electrode system are shown in Figures 2.12 and 2.13.
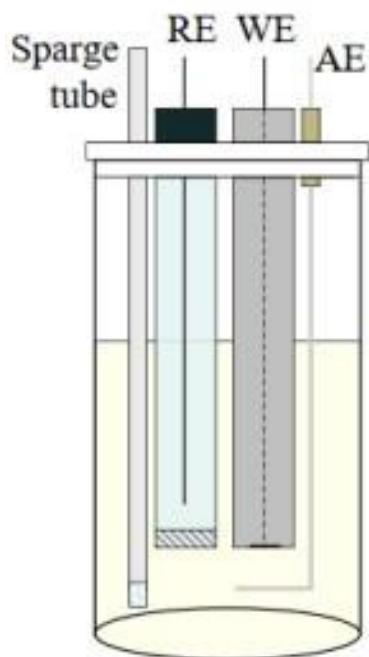
Figure 0.13: Electrochemical cell (Harvey, 2011).
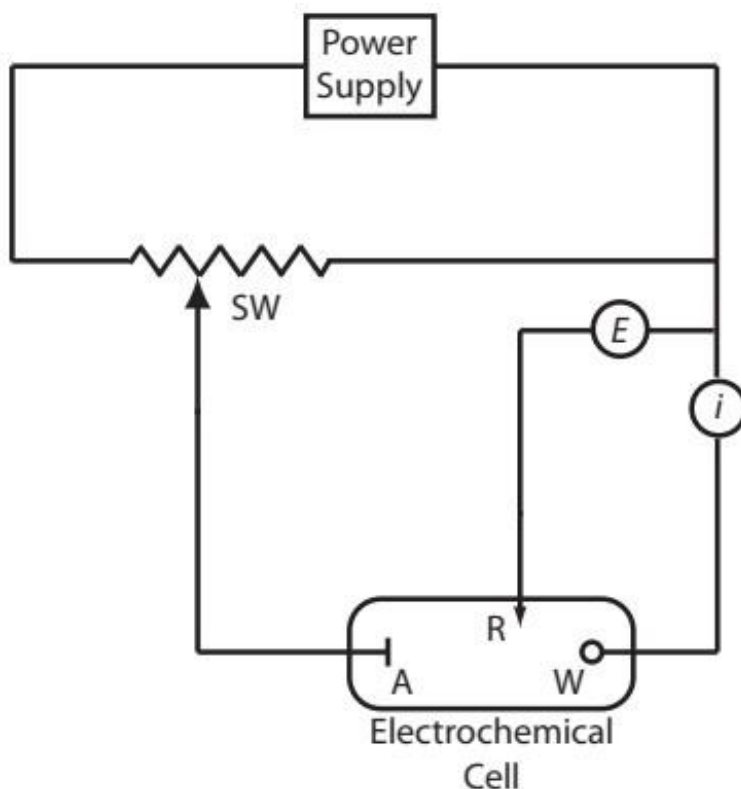
Figure 0.14: A schematic diagram of a three-electrode system potentiostat (Harvey, 2011).

The WE is the most important component of an electrochemical cell, since it is at the interface between WE and the solution that transfer of electrons takes place. It is critical to consider the type and nature of the working electrode (WE) since the experimental success relies on it. The

following factors are usually considered in selecting a WE for electrochemical analysis. Fast reproducible electron transfer and ability of the electrode to perform over a wide potential window, ability of the electrode to be made into different shapes, cost of the material and surface renewal due poisoning after measurement. The most common materials used as a WEs are, mercury, gold, platinum and carbon (and its various forms) (Liang *et al.*, 2013).

Platinum is favoured due to good electrochemical inertness however high cost and its ability to reduce small amounts of acid or water are its disadvantages. Gold electrodes have similar characteristics to those of Platinum but are limited to positive potential range due to surface oxidation, however they are useful in the preparation of modified electrodes especially in fabrication of biosensors (Zhang *et al.*, 2005). Carbon electrodes have a wide negative potential window which make them suitable for scanning to more negative potential compared to gold or platinum, the common carbon electrode is glassy carbon and carbon paste electrode. The dropping mercury electrode (DME) has been extensively utilized in polarography, making it a well-known electrode. The earliest successful electroanalytical detection of electroactive species was achieved through the utilization of polarography, specifically DME polarography (Zuman, 2001). However, the DME has some limitations, including a narrow anodic potential window and its high toxicity. These factors have led to the exploration and development of alternative electrode materials for use in electroanalytical techniques.

In electrochemical measurements, RE electrodes are kept at a constant potential, which is done to vary and control the potential of the WE (e.g., in voltammetry). Some of the common RE are, the Standard Hydrogen Electrode (SHE), silver/silver chloride electrode and the calomel electrode. The SHE was used to establish the electrochemical potential series of elements and it is the basic reference element. However, SHE is difficult to handle in practice. Secondary electrodes are preferred in most experiments. Secondary reference electrodes are metal electrodes coupled to metal salt, e.g., $Ag/AgCl^+$ or $Hg/HgCl$, the metal salt is sparingly soluble with a fixed concentration of the anion. Ideally the reference electrode is placed in the same electrochemical cell together with WE and AE (Inamdar *et al.*, 2009; Stojek, 2010).

Silver/Silver Chloride Electrode (Ag/AgCl) is the most used reference electrode in voltammetry measurements, this is due to its simple construction and well reproducible potential. Ag/AgCl is normally an Ag wire covered with AgCl, fabrication of the electrode have

been described by (Inamdar *et al.*, 2009). Since this reference electrode can be produced in small sizes they have found applications in microsystems (Kitade *et al.*, 2005). Potassium chloride (saturated or 3M) is normally the electrolyte solution in $Ag/AgCl$ RE.
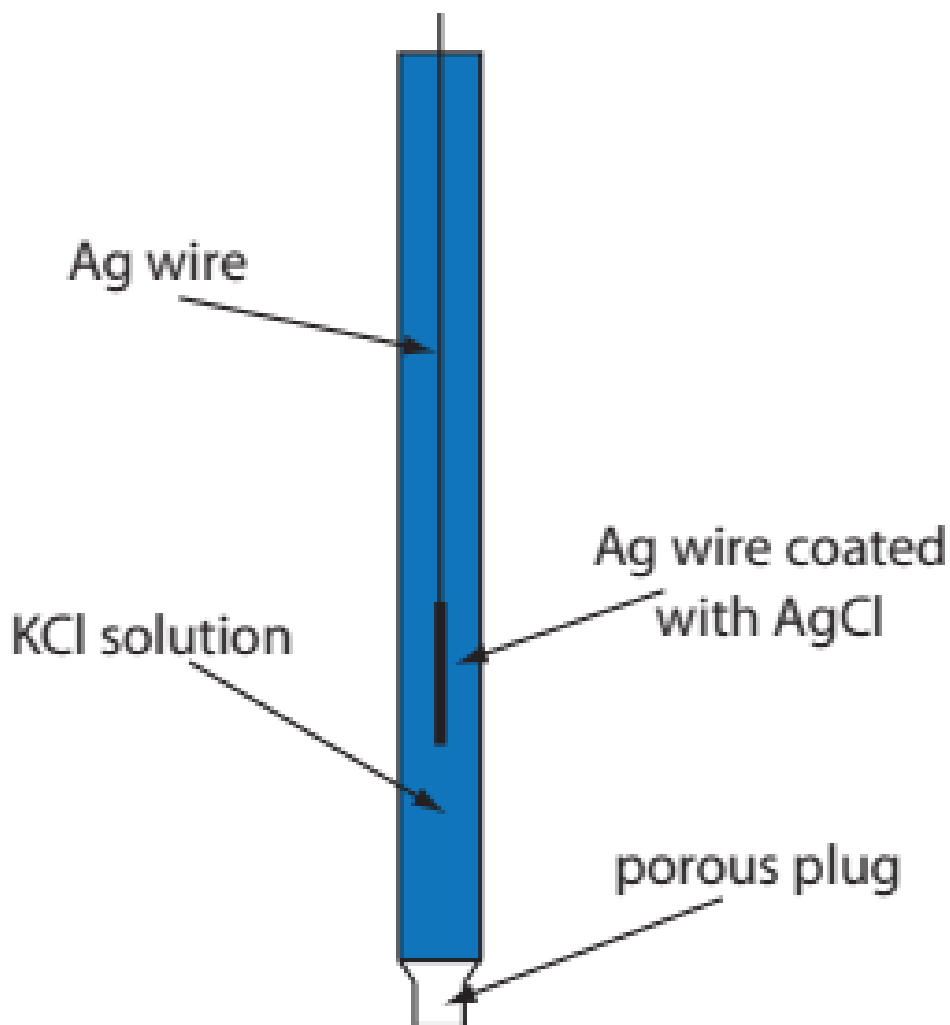
Figure 0.15: Silver / Silver Chloride Reference Electrode (Harvey, 2011)

A high concentration potassium chloride (3M) is also added to the electrochemical cell in order to eliminate migration of electroactive analytes to and from the electrode surface (Harvey, 2011). Supporting electrolyte of high concentration helps to minimise the effect of double layer on the kinetics, increase conduction of the solution by reducing resistance between the WE and the AE (avoiding ohmic drop) (Pletcher *et al.*, 2011).

2.3.3.4: Quantitative analysis in voltammetry

Voltammetric methods have been applied in quantitative analysis of a wide variety of samples which include, environmental samples, pharmaceutical formulations, petroleum samples (gas and oil) among others (Karube *et al.*, 1995). The choice of voltammetric technique depends on the characteristics of the sample e.g., analytes' expected concentration, location and nature of the sample. Pulse techniques have been reported to have precision and accuracy with a limit of detection in the order of 10^{-6} to 10^{-7} M for normal pulse voltammetry , 10^{-7} to 10^{-9} M for differential pulse voltammetry and 10^{-10} to 10^{-12} for stripping voltammetry (Tomková *et al.*, 2018).

In order to calculate the concentration of unknown samples, a standard calibration curve is necessary. For Differential Normal Pulse Voltammetry (DNPV), $\Delta I - E_1$ is the expected curve from the experiment. Using a series of standards differential peak current signal (ΔI_{max}) varies proportionally as the concentration of the analyte, and a plot of ΔI_{max} against standards concentrations will give a calibration curve that can be used to interpolate the concentration of an unknown sample.

2.4:   Method development and validation

Among the objectives of analytical chemistry are, improving established methods, making the established methods more versatile by extending them to other types samples and developing new methods. Once a new method is developed its known as a standard method (Harvey, 2011). The process of documenting and/or proving that a method provides analytical data acceptable for intended purpose is known as method validation (Peters *et al.*, 2007). The goal of method validation is to ensure that future measurements for routine analysis will be close enough (statistically) to the true value for analyte in the sample (Gustavo González and Ángeles Herrador, 2007). Validating a method has been defined as investigating whether the analytical objective of a method has been met, which is obtaining an analytical result with an acceptable uncertainty (Taverniers *et al.*, 2010). Method validation is a requirement for submitting new analytical methods to regulatory agencies such as Environmental Protection Agency (EPA), Food Drug Administration (FDA) among others (Krull and Swartz, 1999). Generally, there are four critical steps in developing a method (Taylor, 1983).

Figure 0.16: Method development steps (Taylor, 1983).

A technique is a scientific principle that is useful for obtaining compositional information about an analyte, for example, spectroscopic or electrochemical technique. A procedure, on the other hand, is a written set of instructions that are essential to implementing a method successfully. Finally, a protocol is a well-defined set of directions that must be followed precisely to achieve reliable and valid analytical results for a specific intended purpose (Taylor, 1983). The procedures for method validations are similar from one method to another, however there are slight differences depending on the analytical technique.

2.4.1: Method validation process

Several renowned organisations and agencies offer guidelines on method validation. Some of these agencies are, Association of Official Analytical Chemists (AOAC), American Society for Testing and Material (ASTM), Food and Agricultural Organization (FAO), The World Health Organization (WHO) and International Union of Pure and Applied Chemistry (IUPAC) (Araujo, 2009). The key criteria for evaluating analytical methods, also known as figures of merits are, selectivity, accuracy, precision, linearity, range, limit of detection, limit of quantitation, ruggedness and robustness (Mitra, 2004).

2.4.1.1: Linear concentration range and linearity

Linearity measures how well a calibration curve follows a straight line, it verifies that the response signal varies linearly as the concentration in the concentration range of sample solutions and standards (Harris, 2010). A common measure of linearity is the square correlation coefficient R^2 also known as coefficient of determination or correlation coefficient r. Correlation coefficient is a statistical concept, it is defined that for a set i^{th} pair of measurement denoted (x_i, y_i), and suppose there are n pairs in total. R is calculated using Equation 2.16.

$$r = \frac{\Sigma(x_i - \bar{x})(y_i - \bar{y})}{\sqrt{\Sigma(x_i - \bar{x})^2 \Sigma(y_i - \bar{y})^2}} \tag{2.16}$$

Where $\bar{x}$ and $\bar{y}$ are the average of x and y measurements respectively. Mathematically r lies between -1 and $+1$ i.e., $(-1 < r < +1)$. If r lies very close to 1 , $r = 0.999$ indicates a

linear relationship between x and y measurements (Miller and Miller, 2010). However, in many instances a scatter plot provides most useful summary of the relationship between x and y.

If there exist a linear relationship between y_i and x_i a linear equation that fits the data pairs (x_i, y_i) of n measurements can be obtained, the process of obtaining this equation is known as curve fitting. This can be done manually by plotting the data on a graph paper and drawing a line of the best fit, however, a better approach is to apply statistics a process known as linear regression analysis. If a straight-line relationship is assumed the data fits a straight-line equation of the form.

$$y = a + bx \qquad (2.17)$$

Where y is the dependent variable (signal), x is the independent variable (concentration), b is the gradient of the line and a is the y intercept. Statistically the best line of fit, is the line through points (x_i, y_i) for which the sum of the squares of the deviations of the points from the line is minimum. The gradient of the straight line, b, and the y-intercept a can be found using Equations 2.18 and 2.19.

$$b = \frac{\Sigma(x_i - \bar{x})(y_i - \bar{y})}{\Sigma(x_i - \bar{x})^2} \qquad (2.18)$$

$$a = \bar{y} - b\,\bar{x} \qquad (2.19)$$

The unknown values of x with known values of y are calculated using equation 2.17, this involves unknown uncertainties in a and b which are propagated in the calculation. The unknown uncertainties are due to random errors in the values of the slope and the intercept. Equations 2.20 is used to calculate the uncertainties in the slope and the intercept i.e., S_b and S_a.

$$S_{\frac{y}{x}} = \frac{\sqrt{\Sigma\,(y_i - \hat{y}_i)}}{n - 2} \qquad (2.20)$$

Where $S_{y/x}$ is the estimate of the random error in the y-direction, $y_i - \hat{y}_i$ is the y-residual, $\hat{y}_i$ points calculated using the regression line corresponding to the individual x-values, $n - 2$ is the degree of freedom. Using $S_{y/x}$, random error estimate for the slope, S_b and for the intercept, S_a can be determined using the following equations (Miller and Miller, 2010).

$$S_b = \frac{S_{\frac{y}{x}}}{\sqrt{\Sigma\,(x_i - \bar{x})^2}} \qquad (2.21)$$

$$S_a = S_{\frac{y}{x}}\sqrt{\frac{\Sigma\,x_i^2}{n\,\Sigma\,(x_i - \bar{x})^2}} \qquad (2.22)$$

Range is a concept related to linearity, there are two type or range: *Linear range,* it is the concentration range of an analyte over which response (signal) is proportional to concentration and which acceptable accuracy and precision are obtained. *Dynamic range*, is the concentration range over which there is a measurable response to analyte concentration although the response is not linear. Linear range is shown in Figure 2.17.
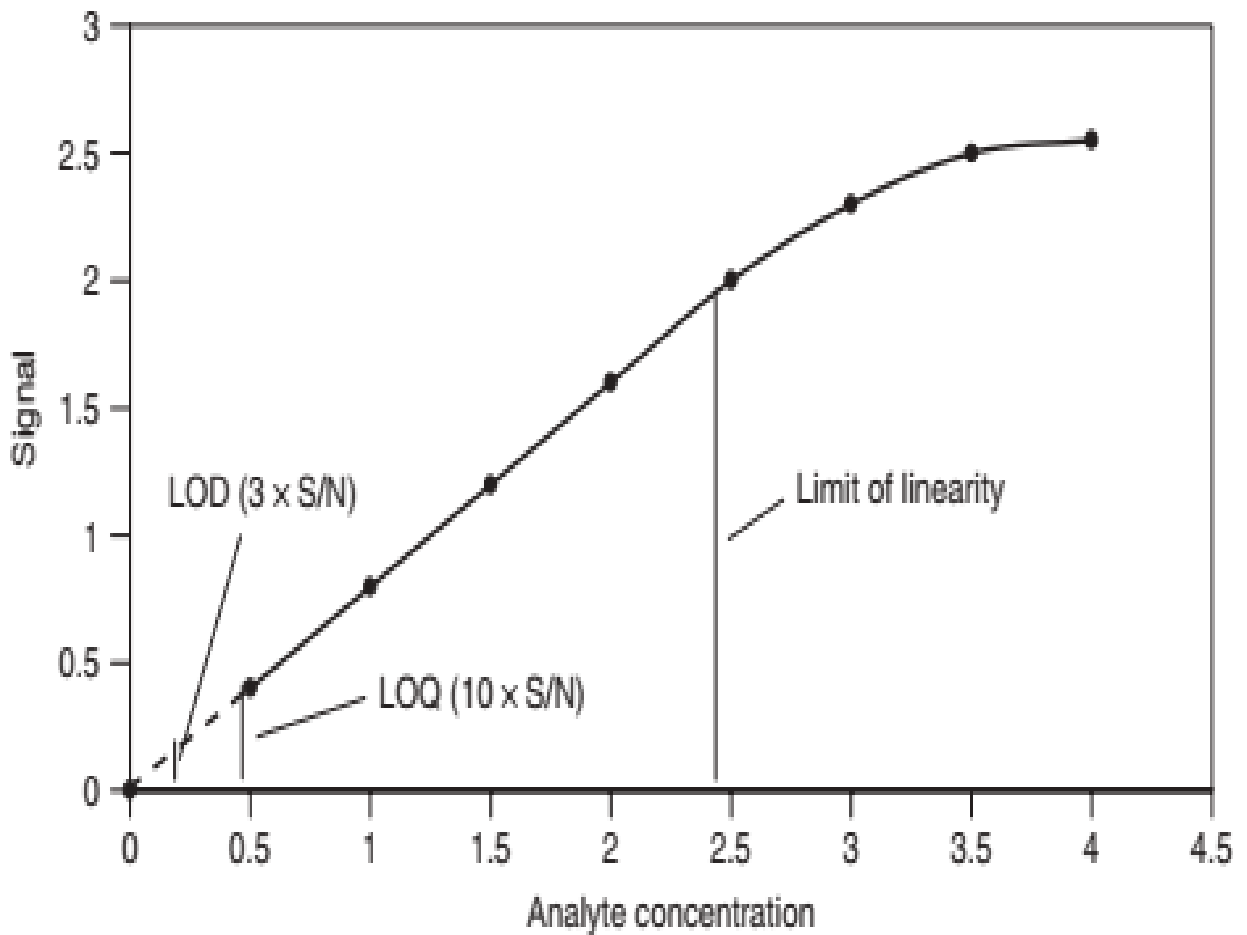
Figure 0.17: A graph showing linear concentration range. (Elizabeth and Victoria, 2007).

32

2.4.1.2: Limit of detection and limit of quantitation

Limit of detection is the lowest concentration level that can be determined to be statistically different from an analyte blank (Evard *et al.*, 2016). A definition by AOAC states that LOD is the lowest content that can be measured with reasonable statistical uncertainty, International Union of Pure and Applied Chemistry (IUPAC) defines it as the smallest amount of concentration of an analyte in a sample that can be reliably distinguished from zero (Shrivastava and Gupta, 2011). A full agreement about the definition between researchers, publishers, regulatory bodies has not been met, however, recent trends define LOD as the analyte concentration giving a signal equal to the blank signal, plus three standard deviations of the blank, S_B (Miller and Miller, 2010).

$$l.o.d = y_B + 3S_B \qquad (2.23)$$

Where y_B, is the blank's signal and s_B is the standard deviation of the blank signals. The value of y_B is estimated by a, y-intercept of the calibration curve, in terms of concentration. Equation 2.23 simplifies to Equation 2.24.

$$L.O.D = \frac{3s_B}{b} \qquad (2.24)$$

Limit of Quantitation is the lowest concentration of an analyte that can be measured at an acceptable level of precision and accuracy, typically a precision of 10 to 20% relative standard deviation (RSD). In absence of a specified precision then the concentration that gives 10 standard deviations above the blank is used (Christian *et al.*, 2014)

$$LOQ = y_B + 10S_B \qquad (2.25)$$

2.4.1.3: Accuracy and precision

Accuracy of a method is defined as the closeness (or nearness) of the measured value to the true value of a sample (Christian *et al.*, 2014), it is also defined as the agreement of a measurement with the true value of the quantity being measured (Willard *et al.*, 1988). Accuracy has also been defined by the International Organization for Standardization (ISO 5725-1) as the closeness of agreement between a test result and the true value (or accepted reference value of the analyte).

Accuracy is determined by spiking a sample with a known concentration of the analyte, and then analysing the sample using the developed method (the method being validated). Accuracy is then measured in terms of percent recovery of the signal against the expected signal. Accuracy is calculated using Equation 2.26.

$$\% \text{ Recovery} = \frac{\text{Observed Result}}{\text{Expected Result}} \times 100 \qquad (2.26)$$

Precision of a method describes how well replicate measurements are in agreement with one another, it is usually expressed in standard deviation (Harris, 2010). Due to random errors in measurements results from as single measurement are usually not accepted as a true value, an estimate of the random errors is necessary in predicting the range that the true value may lie, this is done by carrying out repeated measurements. The average value and the variance of measurement are calculated using Equation 2.27 and Equation 2.28 respectively. The relative standard deviation is then calculated using Equation 2.29.

$$\bar{x} = \frac{\sum x_i}{n} \qquad (2.27)$$

$$s = \sqrt{\frac{\sum (x_i - \bar{x})^2}{n - 1}} \qquad (2.28)$$

$$RSD = \frac{s}{\bar{x}} \ or \ \% \ RSD = \frac{s}{\bar{x}} \times 100 \qquad (2.29)$$

Where $\bar{x}$ is the average value and s is the standard deviation, x_i is the ith measurement, n is the number of measurements, $n - 1$ is known as degrees of freedom (for large samples > 30 , n is taken, and population standard deviation σ calculated). It has been pointed out that accuracy is the most crucial parameter that an analytical method should address (Miller and Miller, 2010).

CHAPTER THREE

MATERIALS AND METHODS

3.1: Chemicals and solutions

The chemicals used in this study were sourced from Loba Chemie Ltd Co. The chemicals used and their purity were: Sulphuric Acid (H_2SO_4) 98% (w/v) (Analytical Reagent) with specific gravity of 1.84g, Ammonium heptamolybdate tetrahydrate ((NH_4)$_6Mo_7O_{24} \cdot 4H_2O$) 99.3% (w/w) (AR), Ascorbic Acid ($C_6H_8O_6$) 99% (w/w) (AR), Antimony potassium tartrate ($K_2Sb_2(C_4H_2O_6)_2$) 99% (w/w) (AR), Potassium dihydrogen orthophosphate anhydrous 99.5% (w/w) (AR).

3.2: Apparatus

Electrochemical analysis was done using CHI 123B Electrochemical potentiostat (CH Instruments USA) with a three-electrode system comprising of a 3 mm diameter glassy carbon electrode (WE), Platinum wire (AE) and Ag/AgCl (RE). An analytical balance of a high degree of precision ($\pm$ 0.0001g) was used to measure the mass of the chemicals. A 10 ml capacity electrochemical cell was used for analytical which was done at room temperature. De-ionized water was obtained using B114 Elga-Star De-ionizer with disposable cartridges. The transfer of micro-litre solutions was done using an adjustable Eppendorf micro-pipette.

3.3: Preparation of solutions

The reagents used in this study were prepared as follows.

3.3.1: Sulphuric acid

2.5 M sulphuric acid (H_2SO_4) was prepared by diluting 68 mL of 98% concentrated sulfuric with deionized water to a final volume of 500 ml.

3.3.2: Ammonium heptamolybdate tetrahydrate

0.016 M ammonium heptamolybdate tetrahydrate ((NH_4)$_6Mo_7O_{24} \cdot 4H_2O$) was prepared by dissolving 20 g of the solid was dissolved in 500 ml deionized water.

3.3.3: Ascorbic acid

0.1 M ascorbic acid ($C_6H_8O_6$) was prepared by dissolving 1.76 g of ascorbic acid in 100ml of deionized water. This solution was prepared as required (due to easily oxidizable nature of ascorbic acid).

3.3.4: Potassium antimony tartrate

0.0004 M of potassium antimony tartrate ($K_2Sb_2(C_4H_2O_6)_2$) was prepared by dissolving 0.2743 g of potassium antimony tartrate in 100 ml deionized water.

3.3.5: Mixed reagent

A "Mixed reagent" was prepared by mixing thoroughly 125 ml of 2.5 M sulphuric acid, 37.5 ml of ammonium molybdate, 75 ml of ascorbic acid solution and 12.5 ml of potassium antimony tartrate solution. This reagent was made up of 50 % sulphuric acid, 15 % ammonium molybdate, 30 % ascorbic acid and 5 % potassium antimony tartrate.

3.3.6: Phosphate standard solution

1000 mg/L phosphate standard stock solution was prepared by dissolving 0.1433 g of potassium dihydrogen phosphate (KH_2PO_4) in 100 ml of deionized water. 100, 50, 25 mg/L of phosphate solutions were prepared by dilution of the stock solution.

3.3.7: Preparation of phosphomolybdate complex

To assess the redox behavior of the phosphomolybdate complex, a solution of 10 mg/L of the complex was prepared by pipetting 4.0 mL of phosphate solution from a 50 mg/L (prepared from 1000 mg/L) into a 25 mL volumetric flask. Then, 4mL of mixed reagent was added followed by deionized water to make to the mark. The following Equations 3.1 and 3.2 demonstrate the formation of phosphomolybdate complex ($PMo_{12}O_{40}^{7-}$) (Kolliopoulos *et al.*, 2015).

$$72H^+ + 7PO_4^{3-} + 12Mo_7O_{24}^{6-} \rightarrow 7PMo_{12}O_{40}^{3-} + 36H_2O \qquad (3.1)$$

$$PMo_{12}O_{40}^{3-} + 2C_6H_8O_6 \rightarrow PMo_{12}O_{40}^{7-} + 2C_6H_6O_6 + 4H^+ \qquad (3.2)$$
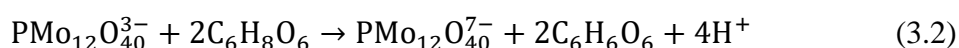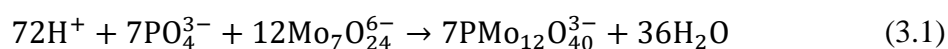
3.4: Analytical techniques

The complex was analysed by Cyclic Voltammetry (CV) and Differential Normal Pulse Voltammetry (DNPV) techniques.

3.5: Preparation of the electrodes

The RE, CE and WE were thoroughly cleaned and rinsed with deionized. Special attention was given in the cleaning process of the WE. The working surface of the glassy carbon was cleaned using 0.3-micron alumina slurry on a polishing pad and then followed by 0.1-micron alumina slurry for about 2 minutes, to obtain a mirror finish of the glassy carbon. This was done before commencement of every experiment. CV and DNPV experiments were done at a temperature of 24 ± 0.1 °C.

3.6: Instrument set up procedure

The procedure for operating the potentiostat model CHI123 from CHI Instruments, USA were used for both CV and DNPV studies. The instrument was switched on and given some time to initialize before running the CHI123 software installed in the computer. The potential window and the operating settings of CV and DNPV were selected using CHI123 software.

Cyclic Voltammetric (CV) and Differential Normal Pulse Voltammetric (DNPV) studies were done using CHI 123B Potentiostat from CHI instruments company, USA. The reference electrode (RE) was made up of silver/silver chloride (Ag/AgCl) electrode with chloride concentration of 4 M, the counter electrode (CE) was made of platinum wire of a diameter 0.04 cm and the working electrode (WE) made up of glassy carbon of diameter 0.30 cm and a surface of 0.071 cm^2. The electrochemical cell used was designed to hold the three electrodes concurrently had a capacity of 10 mL (100 μL). The electrodes were positioned in such a manner that the tips were close to one another to allow for efficient electron transfer between the CE and WE.

3.7: Optimization of analytical techniques

10 mL of the phosphomolybdate complex prepared was then transferred into the quartz electrochemical cell for analysis. Cyclic voltammetry (CV) and Differential Normal Pulse Voltammetry (DNPV) techniques were used. Selection of electrochemical technique and input of electrochemical parameters and collection of data from the potentiostat was facilitated by a

graphical software. Optimization of CV and DNPV techniques were done by selecting electrochemical parameters so as to obtain the best sensitivity. Optimization of the electrochemical parameters, such as, initial potential (V), final potential (V), increment potential (V), amplitude (V), 1st pulse width (sec), 2nd pulse width (sec), sample width (sec), pulse period (sec), quiet time (sec) and sensitivity (A/V) were done through the graphical software of the potentiostat. Optimization involved selecting variables at a high and low value and then combining those variables which give a high response.

3.8: Validation of method

In order to validate the DNPV method in terms of Linear Concentration Range (LCR), Limit of Detection (LOD), Limit of Quantitation (LOQ), calibration standards containing 0, 2, 4, 6, 8, and 10 mg/L of phosphomolybdate complex were prepared by pipetting 0, 1.0, 2.0, 3.0, 4.0, and 5.0 mL from 50 mg/L of PO_4^{3-} solution into 25 ml volumetric flasks, 4 mL of "mixed reagent" was then added to each flask and made to volume with deionized water. The solution was left for about 10 minutes for the complex to form. The voltammograms of the calibration standards were then recorded. Experiments were done in triplicates.

In the determination of accuracy, a 2 mg/L phosphate standard was prepared, then phosphate standard was spiked with 50%, 100% and 150% of the 2 mg/L phosphate standard (a method known as spiking and recovery). To determine the precision, 10 replicate measurements of 4 mg/L of phosphate were made.   The stability of phosphomolybdate complex was determined by measuring peak current of 8 mg/L of phosphomolybdate complex at duration of 1, 5, 10, and 15 min immediately after reacting phosphate with mixed reagent.

3.9: Evaluation of method

Fifty water samples were randomly collected from L. Naivasha. The samples were collected in 50 mL precleaned plastic water bottles then transported to Chiromo Campus, University of Nairobi. The water was then stored in a freezer for subsequent analysis.

20 mL of collected water sample were filtered and then transferred into 25 mL volumetric flask, 4 mL of mixed reagent was then added, and finally made to the mark by deionized water. After 10 minutes, 10 mL of the sample was transferred into an electrochemical cell and analysed using DNPV method.

The output data from the electrochemical analyses was recorded in comma separated values (csv) files. The csv files contained current and potential data, in order to visualize the data, the data in csv files were used to plot voltammograms. Voltammograms plotted, were then used for analysis of results obtained. Voltammograms were prepared using LaTeX document preparation software and data analysed using Microsoft Excel Version 2021.

CHAPTER FOUR

RESULTS AND DISCUSSION

4.1: Optimization of DNPV technique variables for determination of phosphates

The variables: 1st amplitude and 2nd pulse widths, sampling width, pulse period and quiet time were optimized by using the graphical software of the potentiostat. The purpose of optimization was to achieve the best variables for use in the determination of the phosphates. Further it enables one to obtain the optimal values for the parameters such a combination that could give a well-defined response of the complex being determined. The optimized variables were then used for DNPV analysis of the phosphomolybdate complex. The optimized values are presented in Table 4.1

Table 0.1: Differential Normal Pulse Voltammetry variables

Parameter	Value
Init E (V)	-0.6
Final E (V)	2.4
Increment E (V)	0.001
Amplitude (V)	0.05
1st Pulse Width (sec)	0.01
2nd Pulse Width (sec)	0.01
Sample Width (sec)	0.001
Pulse Period (sec)	0.01
Quiet Time (sec)	1
Sensitivity (A/V)	0.01

4.2: Redox behaviour of phosphomolybdate complex during voltammetric analysis

The voltammograms for the redox behaviour of phosphomolybdate complex during determination by Differential Normal Pulse Voltammetry (DNPV) and Cyclic Voltammetry (CV) are presented and discussed in the following sub-sections.

4.2.1: Redox behaviour of phosphomolybdate complex during DNPV assessment

The DNPV voltammograms of the reactants and the complex were recorded as shown in Figures 4.1. and 4.2. DNPV scans were done between a potential window of -0.6 to 2.4 V. The voltammograms of the reactants, ascorbic acid, potassium antimony tartrate and ammonium molybdate did not show any peaks, however sulphuric acid showed several peaks, these peaks were attributed to electrolysis of water. When phosphate was added to the reactants, phosphomolybdate complex was formed and a peak was observed at the potential 0.33V as shown in Figure 4.2.
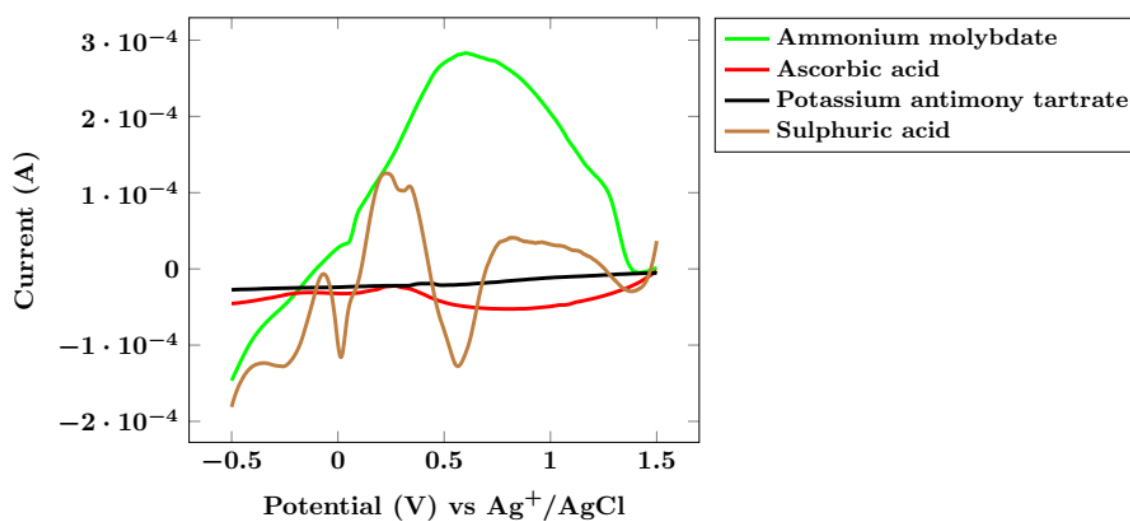
Figure 0.1: Voltammograms of reactants on glassy carbon electrode, ammonium molybdate (0.016M), ascorbic acid (0.1M), potassium antimony tartrate (0.0004M) and sulphuric acid (2.5M).
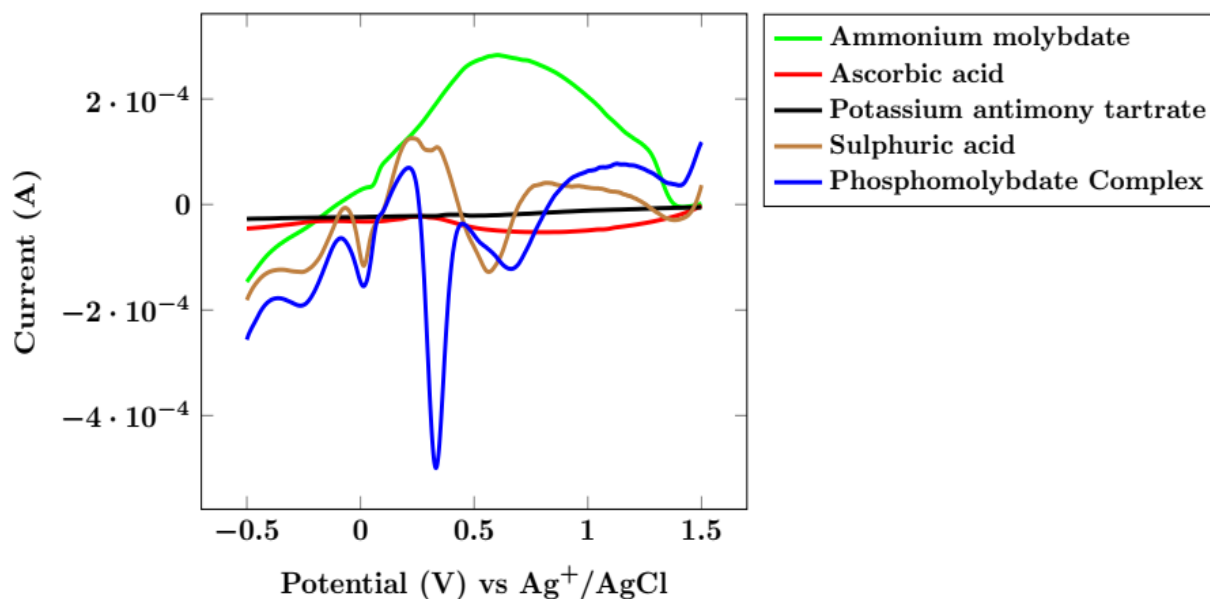
Figure 0.2: Voltammograms of reactants and phosphomolybdate complex. Phosphomolybdate complex formed by 50% sulphuric acid, 15% ammonium molybdate, 30% ascorbic acid and 5% potassium antimony tartrate.

When the concentration of phosphomolybdate complex was altered by increasing the complex concentration through spiking with phosphate solution, there was a change in voltammogram peak heights which depended on the complex concentration according to Figure 4.3.
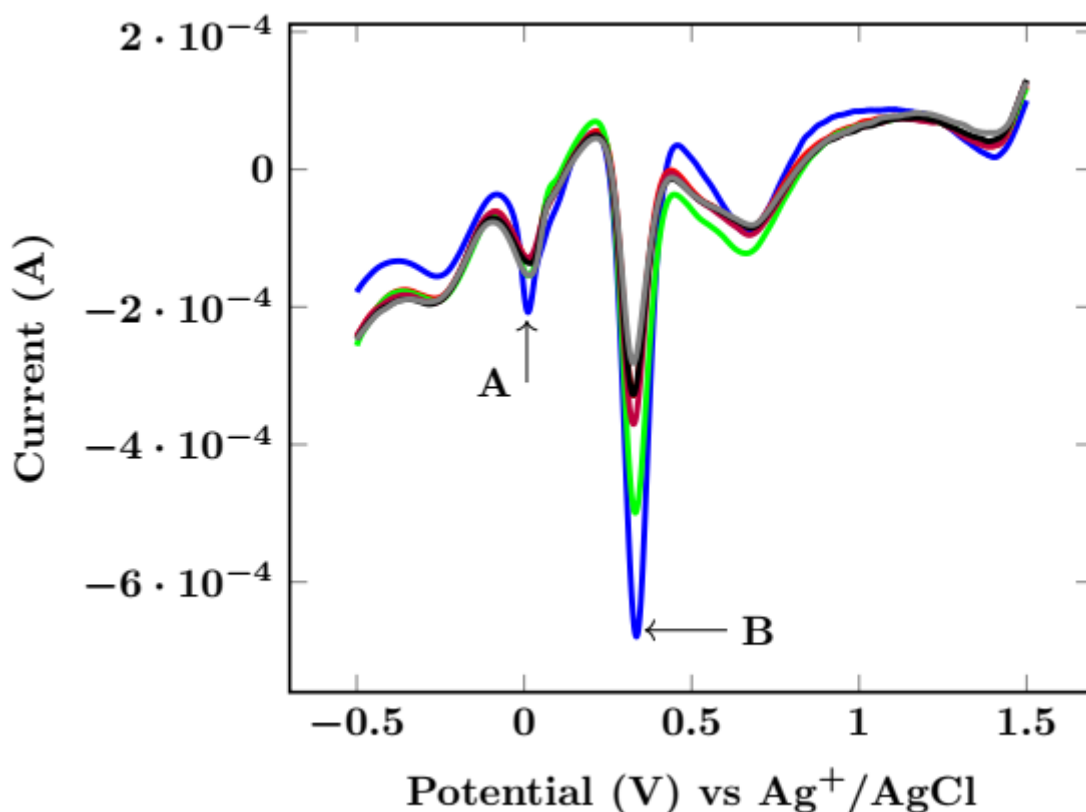
Figure 0.3: Voltammograms of phosphomolybdate complex at different concentrations. Peaks A and B were observed at redox potentials of 0.02V and 0.33V respectively.

The other peaks did not show any increase in peak height as phosphate concentration increased, hence they were not due to the formation of the complex. Both peaks were observed between 0 to 0.5 V potential. Peak A at 0.02 V and peak B at 0.33V provided DNPV redox potentials of phosphomolybdate complex.

4.2.2: Redox behaviour of phosphomolybdate complex when assessed by CV technique.

The cyclic voltammograms of reactants on glassy carbon electrode are presented in Figure 4.4 and the voltammograms for the phosphomolybdate complex are presented in Figure 4.5. The background voltammograms of reactants, ammonium molybdate, ascorbic acid, potassium antimony tartrate and sulphuric acid were obtained. The potential window for CV was -0.24 – 1.0 V, a scan rate of 0.2 V/s, a sampling interval potential of 0.001 V and a quiet time of 2 seconds. The voltammograms of the reactants were obtained so as to distinguish phosphomolybdate complex peak from those of the reactants.
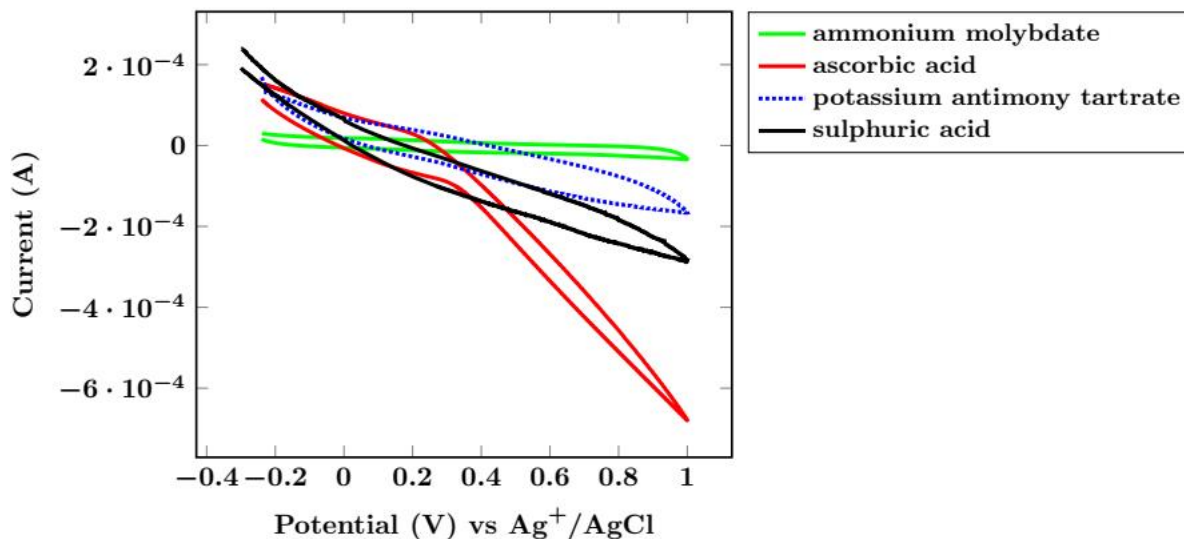
Figure 0.4: Cyclic voltammograms of reactants on glassy carbon electrode. Ammonium molybdate (0.016M), ascorbic acid (0.1M), potassium antimony tartrate (0.0004M) and sulphuric acid (2.5M) at 0.2V/s scan rate.
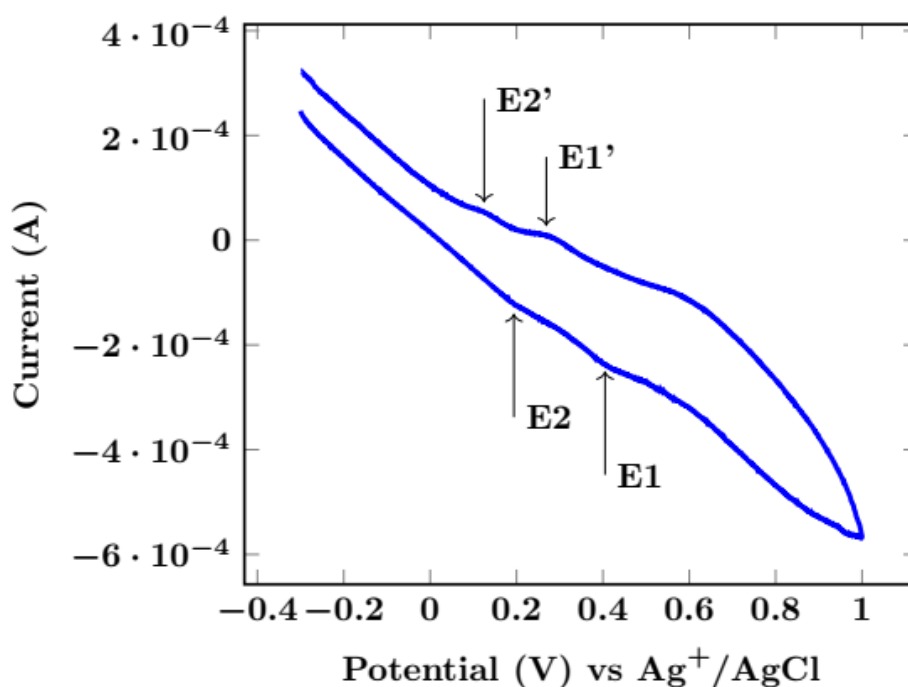
Figure 0.5: Cyclic Voltammograms of phosphomolybdate complex formed by 10mg/L phosphate reaction with 50% sulphuric acid, 15% ammonium molybdate, 30% ascorbic acid and 5% potassium antimony tartrate at 0.2V/s scan rate.

The cyclic voltammograms of the reactants: ammonium molybdate, potassium antimony tartrate, and sulphuric acid (Figure 4.4) did not show any peaks indicating that these reagents were not redox active. However, the CV for ascorbic acid showed a single broad peak between

44

potentials 0.2 and 0.4V. Zare and Nasirizadeh, (2010) have reported ascorbic acid to have an oxidation peak between potentials 0.3 and 0.4V , therefore this peak is attributed to oxidation of ascorbic acid at the working electrode.

The cyclic voltammogram of Phosphomolybdate complex ($PMo_{12}O_{40}^{7-}$) showed two reduction peaks and two oxidation peaks (Figure 4.5). The reduction peaks were observed at potentials 0.43V and 0.21V and oxidation peaks at 0.28 V and 0.13 V. Phosphate is made electroactive through a reaction with molybdate salts to form a complex which makes its electrochemical detection possible as outlined in Equations 3.1 and 3.2 (Jońca *et al.*, 2013).

The two peaks shown in Figure 4.5 that were observed during both cycles indicated that phosphomolybdate complex has two redox centres. These redox centres are due to oxidation of phosphomolybdate complex at the working electrode (WE). The oxidation process takes place at the molybdenum metal ion. The peaks observed are due to oxidation of $PMo_{12}O_{40}^{7-}$ complex, and reduction process that occurs in two stages. In the first peak Mo(VI) is reduced to Mo(IV) while the second peak is due to the reduction of Mo(IV) to Mo(II) (Wang *et al.*, 2014).

When the redox potentials of peaks A and B obtained using DNPV (*section 4.2.1*) were compared with the Cyclic Voltammetry (CV) peaks of the complex, it was observed that CV of the complex had two peaks whose formal redox potentials were 0.36 V and 0.17 V. The study revealed that the formal redox potential of 0.36V correlated with the DNPV peak B whose potential was 0.33 V.

4.2.2.1: Electrochemical characteristics of phosphomolybdate complex.

The cyclic voltammograms of $PMo_{12}O_{40}^{7-}$ complex was used to deduce information about formal redox potentials, electron transfer, equilibrium constant (K_{eq}) and diffusion coefficient (D) of the complex. The evaluation of the above characteristics were obtained as follows.

Formal redox potential

The oxidation potentials (anodic redox potentials) occurred at $E_1 = 0.4340$ and $E_2 = 0.2078\ V$ potentials while the reduction potential (cathodic redox potentials) for the reverse cycle occurred at $E_1' = 0.2797\ V$ and $E_2' = 0.1271\ V$ potentials as shown in Figure 4.6. The formal redox potential was then calculated by taking the average of anodic peak potential (E_{pa}) and the cathodic peak potential (E_{pc}) according to Equation 4.1 (Kissinger and Heineman, 1983)

$$E^0 = \frac{E_{pa} + E_{pc}}{2} \tag{4.1}$$

E^0 for E_1 was evaluated by taking the average of E_a and E_c.

$$E^0 = \frac{0.4340 + 0.2797}{2} = 0.35685\ V$$

Similarly, E^0 for E_2 was also calculated

$$E^0 = \frac{0.2078 + 0.1271}{2} = 0.16745\ V$$

The formal redox potentials E^0 for the two redox centres of the complex were found to be 0.357V and 0.167V.

Song *et al.*, (2016) using Linear Scan Voltammetry reported two reduction peaks of the complex at 0.25V and at 0.15V corresponding to reduction of Mo(VI) →Mo(IV) and Mo(IV) → Mo(II) respectively. Analysis of the complex by Kolliopoulos *et al.*, (2015) using Cyclic Voltammetry showed that reduction peaks were observed at 0.27 V and 0.13 V while oxidation peaks were observed at 0.16V for oxidation of Mo(II) → Mo(IV) and 0.30 V for oxidation of Mo(IV) → Mo(VI). In this study, the reduction potential was observed at 0.28 V and 0.13 V for Mo(VI) →Mo(IV) and Mo(IV) → Mo(II) respectively. The results compared well with reduction potentials reported by Song *et al.*, (2016) and by Kolliopoulos *et al.*, (2015)

The reduction potentials of the phosphomolybdate complex obtained in this study showed a strong correlation with studies by Song *et al.*, (2016) and Kolliopoulos *et al.*, (2015). This was an affirmation that the peaks produced by CV was indeed that of the phosphomolybdate complex.

Electron transfer

Phosphomolybdate complex is a Keggin ion with the formula $PMo_{12}O_{40}^{7-}$ (Son *et al.*, 2013). This complex is formed by two reactions according to Equation 3.1 and Equation 3.2. The addition of ascorbic acid and antimony tartrate reduces $7PMo_{12}O_{40}^{3-}$ to $PMo_{12}O_{40}^{7-}$ according to Equation 4.2.

$$PMo_{12}O_{40}^{3-} + 2e^- \rightarrow PMo_{10}^{6+}Mo_2^{5+}O_{40}^{3-} \tag{4.2}$$
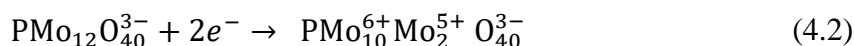
This reaction produces a complex $PMo_{10}^{6+}Mo_2^{5+}O_{40}^{3-}$ in which Mo is in a mixed oxidation state of +6 and +5. The process involve 2 electrons (Cinti *et al.*, 2016).

Equilibrium constant (K_{eq})

Equilibrium constant of the reaction processes was calculated from Nernst Equation given in Equation 4.3.

$$E = E^0 - \frac{RT}{nF} \ln \frac{[R]}{[O]} \tag{4.3}$$

At standard temperature, $T = 298K$, Nernst equation becomes:

$$E = E^0 - \frac{0.0592}{n} \log Q \tag{4.4}$$

where Q is the reaction quotient. As the redox reaction proceeds ($Ox + ne^- \rightarrow R$), Ox reduces, and R increases however as this happens the cell potential gradually decreases until the reaction is at equilibrium. At equilibrium the reaction quotient $Q = K_{eq}$, and the cell potential, E=0 then the Nernst equation becomes:

$$0 = E^0 - \frac{0.0592}{n} \log K_{eq}$$

$$E^0 = \frac{0.0592}{n} \log K_{eq}$$

$$\log K_{eq} = \frac{nE^0}{0.0592} \tag{4.5}$$

K_{eq} can then be calculated by taking the antilog of $\frac{nE^0}{0.0592}$. By taking formal redox potentials E^0, 0.357V and 0.167 V, K_{eq} for each potential was calculated K_{eq}. The value of n for the two processes is 2. The values for the equilibrium constants are presented in Table 4.2.

Table 0.2: Equilibrium Constant Values for Phosphomolybdate complex

E^0	N	$log\ K_{eq}$	K_{eq}
0.357	2	12.06	1.15×10^{12}
0.167	2	5.64	4.36×10^5

The values for K_{eq} are usually proportional to the standard potential of the reaction, therefore, a value of $K_{eq} > 1$ reaction favours reduced species (favours product formation) (Thompson and Kateley, 1999).

From the data obtained, the K_{eq} value for the first and second redox centres were found to be 1.15×10^{12} and 4.36×10^5 respectively, this meant that the reduction of $Mo(IV) \rightarrow Mo(II)$ is highly favoured than the reduction of $Mo(VI) \rightarrow Mo(IV)$ and that the reduced species $Mo(II)$ is stable compared to $Mo(IV)$.

Diffusion coefficient (D)

Another important information that can be deduced from Cyclic Voltammetry is diffusion coefficient, D, of a redox active species. In order to find D, voltammograms of the complex at different scan rates were recorded. Scan rates controlled how fast the applied potential is scanned, hence high scan rates lead to decreased diffusion layer and therefore high currents are observed. For a reversible electron process, Randles-Sevcik equation (Equation 4.6) describes a linear relationship between the increasing peak current (i_p) and the square root of the scan rate (Vs^{-1}) (Elgrishi *et al.*, 2018).

$$i_p = (2.69 \times 10^5)n^{3/2}AD^{1/2}Cv^{1/2} \tag{4.6}$$

The cyclic voltammograms at different scan rates are shown in Figure 4.6
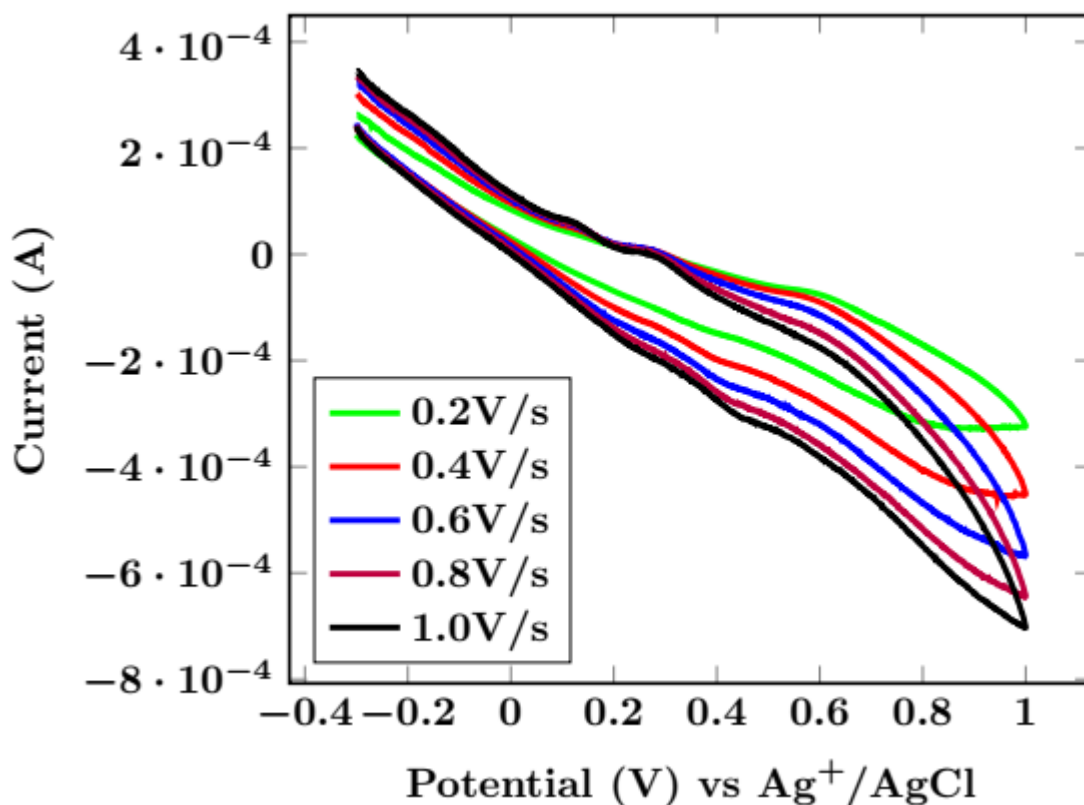
Figure 0.6: Cyclic Voltammograms of phosphomolybdate complex at varying scan rates formed by 10mg/L phosphate solution with 50% sulphuric acid, 15% ammonium molybdate, 30% ascorbic acid and 5% potassium antimony tartrate.

Peak currents at E_1 (0.43V) and E_2 (0.21V) at different scan rates as shown in Table 4.3 were used to plot graphs of i_p versus square root of scan rate shown in Figures 4.7 and 4.8.

Table 0.3: Peak currents at different scan rates

Scan rate (V/s)	Scan rate square root	E_1 (0.43V) Peak Current (A)	E_2 (0.21V) Peak Current, (A)
0.2	0.447214	0.000291	1.05E-05
0.3	0.547723	0.000321	1.13E-05
0.4	0.632456	0.000342	1.30E-05
0.5	0.707107	0.000433	1.58E-05
0.6	0.774597	0.000435	1.88E-05
0.8	0.894427	0.000544	2.27E-05
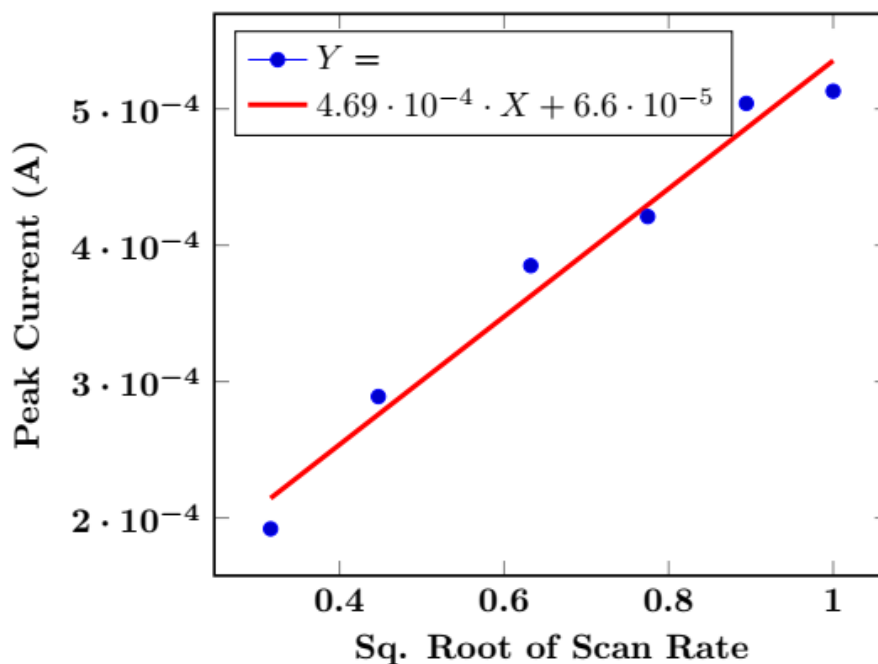
Figure 0.7: Peak current against square root of scan rate, for a redox centre at 0.43V corresponding to reduction of Mo (VI) → Mo (IV), the linear relationship is Y=4.69 $\cdot 10^{-4}$ X + 6.6 $\cdot$ 10^{-5} and r= 0.9914
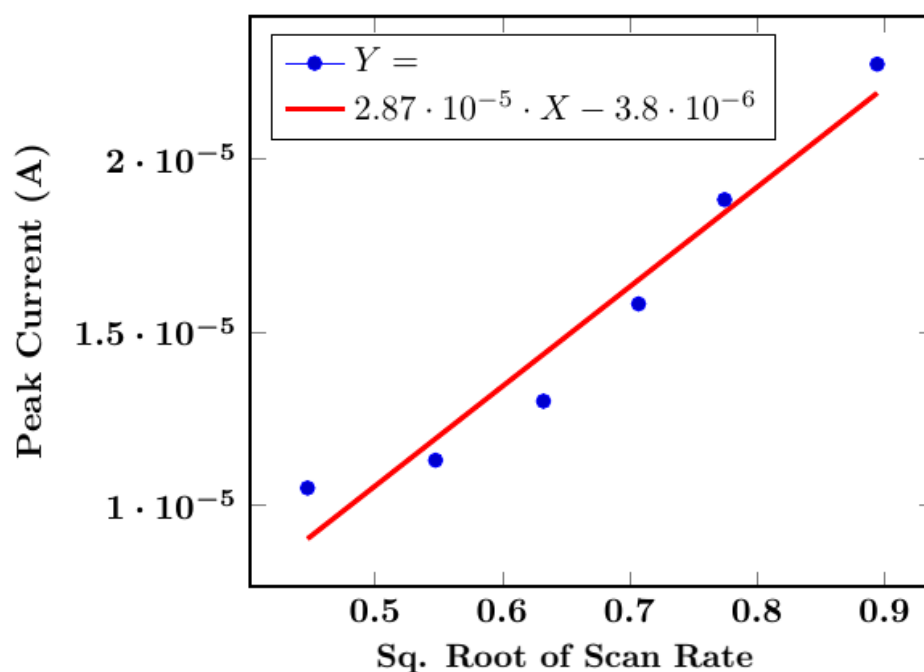
Figure 0.8: Peak current against square root of scan rate, for a redox centre at 0.21V corresponding to reduction of Mo (IV) → Mo (II), the linear relationship is Y=2.87 $\cdot 10^{-5}$ X + 3.8 $\cdot$ 10^{-6} and r= 0.9743.

Figures 4.7 and 4.8 showed that there was a strong linearity for peak current against root scan rate, with a linear regression $r = 0.9914$ and $r = 0.9638$ respectively which indicated that phosphomolybdate complex is a freely diffusing redox species.

Applying Randles-Sevcik equation (Equation 4.7) the slope (or gradient) of curve obtained from a plot of i_p (in amperes) against $v^{1/2}$ (in $\sqrt{V/s}$) is equivalent to $(2.69 \times 10^5)n^{3/2}AD^{1/2}C$. Where n is the number of electrons, A is the surface area of the working electrode, D is the diffusion coefficient and C is concentration of the analyte. The Diffusion coefficient D can be calculated from the expression.

$$i_p = (2.69 \times 10^5)n^{3/2}AD^{1/2}Cv^{1/2}$$

$$D^{\frac{1}{2}} = \frac{slope}{(2.69 \times 10^5)n^{\frac{3}{2}}AC} \tag{4.7}$$

$$D = \left(D^{\frac{1}{2}}\right)^2$$

The glassy carbon electrode had a diameter of 0.3 cm, hence the area $A = 0.0706858\ cm^2$. The number of electrons $n = 2$ due to reduction of Mo, from Mo(VI) to Mo(1V), the concentration of the complex was obtained from the stoichiometric equation below.

$$72H^+ + 7PO_4^{3-} + 12Mo_7O_{24}^{6-} \rightarrow 7PMo_{12}O_{40}^{3-} + 36H_2O$$
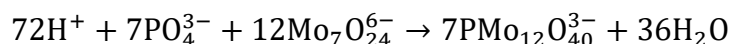
7 moles of PO_4^{3-} reacts with 12 moles of $Mo_7O_{21}^{6-}$ to form 7 moles of $PMo_{12}O_{40}^{3-}$. The concentration of PO_4^{3-} used was 10mg/L which is equivalent to 0.105 mmol/L, therefore the concentration of the complex was $7 \times 0.105 = 7.35\ mmol/L$. Therefore, to obtain D in cm^2s^{-1} it is necessary to convert the concentration to $mol\ /cm^3$, hence $C = 7.35 \times 10^{-7}\ mol\ /cm^3$.

From the graph shown in Figure 4.7, the slope of the curve was found to be $0.000469\ AV^{1/2}s^{-1/2}$, Diffusion coefficient was then determined using Equation 4.9.

$$D^{1/2} = \frac{0.000469}{(2.69 \times 10^5) \times (2)^{3/2} \times 0.0706858 \times 7.35 \times 10^{-7}} = \frac{0.000469}{0.03953}$$

$$D^{1/2} = 0.011864$$

$$D = \left(D^{\frac{1}{2}}\right)^2 = (0.011864)^2 = 1.408 \times 10^{-4}\ cm^2s^{-1}$$

Similarly, for reduction of Mo(IV) $\rightarrow$ Mo(II), D was calculated and found to be $5.271 \times 10^{-7}\ cm^2 s^{-1}$. In comparison, D for reduction of Mo(IV) $\rightarrow$ Mo(II) was found to be smaller compared to that of reduction of Mo(VI) $\rightarrow$ Mo(IV). When compared to diffusion coefficient of a smaller molecule (low molecular weight) such as potassium ferric cyanide which has a D value of $6.35 \times 10^{-6} cm^2 s^{-1}$ (Arvía *et al.*, 1967), the determined D value of $1.408 \times 10^{-4}\ cm^2 s^{-1}$ was found to be large, however the D value of $5.271 \times 10^{-7} cm^2 s^{-1}$ was found to be small. Factors that can impact the diffusion coefficient include the size and shape of the molecule (Song and Cabooter, 2017), the viscosity of the medium through which the molecule is diffusing, and the concentration gradient of the molecule (Bakhtiari and Ghalami-Choobar, 2015).

4.3:   Validation of the differential normal pulse voltammetric method

Validation of DNPV method was done by determining: linear concentration range (LCR), limit of detection (LOD), limit of quantitation (LOQ), accuracy and precision. Voltammograms for validation of LCR, LOD and LOQ were obtained at varying concentrations of phosphomolybdate complex as shown in Figure 4.9. The DNPV voltammograms were obtained between 0.0 V and 0.2 V potential. The phosphomolybdate peak chosen for validation of the method was a peak between 0.0 V and 0.2 V, this is because this peak was well defined, the peak height could be easily be determined and at low concentration the peaks of the standards were well resolved.

The peak heights of the voltammograms increased with increase in phosphate concentration, with the smallest peak height corresponding to the blank concentration and the largest peak height corresponding to 8 mg/L phosphate concentration. The corresponding current signals were negative, however, the absolute value of the peak currents as recorded in Table 4.4 were used to plot a calibration a standard calibration curve as shown in Figure 4.10.
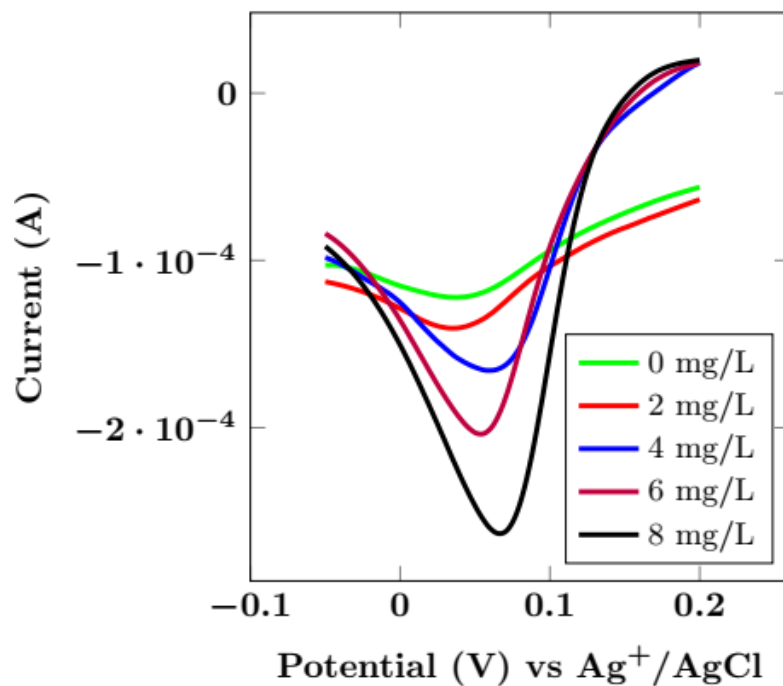
Figure 0.9: DNPV Voltammograms of 0, 2, 4, 6, and 8 mg/L phosphate concentration.

Table 0.4: Change in peak currents when phosphate concentration is varied

Concentration (mg/L)	Peak Current (A)
0	0.0001227
2	0.0001414
4	0.0001798
6	0.0002041
8	0.0002637
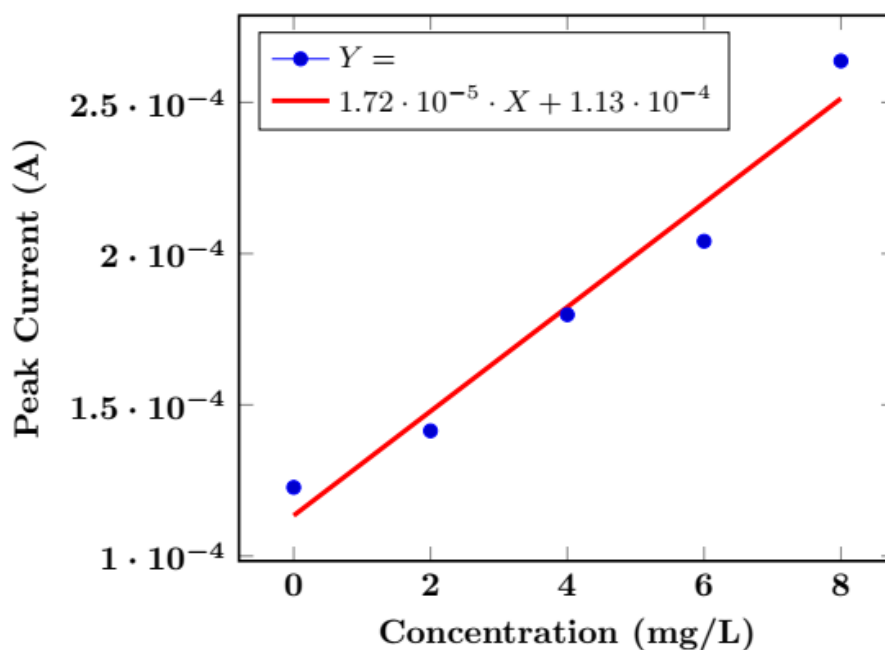
Figure 0.10: Standard calibration curve of peak current against phosphate concentration, the linear equation is Y=1.7235 × 10^{-5} X + 0.0001134, and r=0.9816

A standard calibration curve was prepared in order to check visually the linear relationship between peak current and phosphate concentration. From the linear relationship, the slope, the y-intercept and the linear regression equation were determined. The standard calibration curve was then used to determine LOD, LOQ and phosphate concentration of collected water samples.

4.3.1: Standard calibration and linearity

From the standard calibration curve, a linear concentration range was observed from 0 to 8 mg/L, with the largest peak current corresponding to 8 mg/L phosphate concentration. It was noted that the curve was not linear for phosphate concentration of 10 mg/L and greater. Results in Table 4.4 were used to calculate the calibration curve statistics.

The value r was found to be equal to 0.9816 which indicated that there is a strong linear correlation between the signal response and concentration. The linear regression equation of y on x i.e., was found to be $y = 1.7235 \times 10^{-5} X + 0.0001134$. The linear regression equation is usually used to estimate concentration of test samples and therefore it is important to calculate the random errors on the slope and on the y intercept. The standard error of y on x, $s_{y/x}$, was found to be 1.2256×10^{-5} and the confidence limits for a and b were found to be

$0.0001134 \pm 3.0212 \times 10^{-5}$ and $1.7235 \times 10^{-5} \pm 6.1669 \times 10^{-6}$ respectively. The calibration curve statistical calculations provided information about linearity, linear regression equation and the random errors in estimation of the slope and the y-intercept, information that is necessary in order to determine the limit of detection/quantitation and quantify phosphate concentration of test samples. The linear calibration equation had a slope $b = 1.725 \times 10^{-5}$ with an associated error of 6.1669×10^{-6}, and with an intercept of $a = 0.0001134$ with an error of 3.0212×10^{-5}. The values 6.1669×10^{-6} and 3.0212×10^{-5} were uncertainties associated with the calibration curve.

4.3.2: Limit of detection and limit of quantitation

Limit of Detection (LOD) of an analytical method is the smallest amount of an analyte in a sample which can be detected. LOD was calculated using Equation 4.8.

$$L.O.D = \frac{3s_B}{b} \qquad (4.8)$$

Where b, is the slope of the calibration curve and s_B is the standard deviation of the blank. Therefore,

$$L.O.D = \frac{3 \times 3.7834 \times 10^{-7}}{1.7235 \times 10^{-5}} = 0.06586 \, mg/L$$

Similarly, Limit of quantitation (LOQ) can also be determined. LOQ is regarded as the lower limit for precise quantitative measurements, LOQ was calculated using Equation 4.9.

$$L.O.Q = \frac{10s_B}{b} \qquad (4.9)$$

LOQ was found to be $0.21952 \, mg/L$.

LOD of the method was found to be $0.06586 \, mg/L$, which meant that the lowest concentration of phosphate that the developed method could reliably detect is 0.06586 mg/L, i.e., the concentration that is significantly different from the blank. LOQ was found to be $0.21952 \, mg/L$, this meant that, $0.21952 \, mg/L$ phosphate concentration is the lowest amount that could be quantitatively determined with a suitable precision.

Limit of detection of the standard method (UV-Vis spectrophotometry) for analysis of phosphates in water has been reported to be $0.010 \, mg/L$ (Baird *et al.*, 2017). Linear Scan Voltammetry (LSV) has also been used to determine phosphates with a limit of detection of $4.0 \, \mu g/L$ (Song *et al.*, 2016). This method employs a gold working electrode, Ag/AgCl/Cl⁻ reference electrode and a platinum counter electrode. Cyclic Voltammetry has also been

applied in analysis of phosphate with a detection limit of 0.3 $\mu g/L$, (Kolliopoulos *et al.*, 2015). The method used screen-printed graphite electrode, screen printed $Ag/AgCl$ paste and a screen-printed counter electrode. These methods have a lower limit of detection compared to the DNPV method developed. The difference in limit of detection between LSV, CV and the developed method could be attributed to different working electrodes employed, modified reagents and experimental conditions.

4.3.3: Accuracy and precision

The accuracy of the method was determined by spiking a 2 mg/L (original) phosphate standard with different amounts of additional phosphate, specifically 50%, 100%, and 150% of the of 2 mg/L. Figure 4.11 shows the voltammograms that were obtained and Table 4.5 shows the corresponding peak currents.
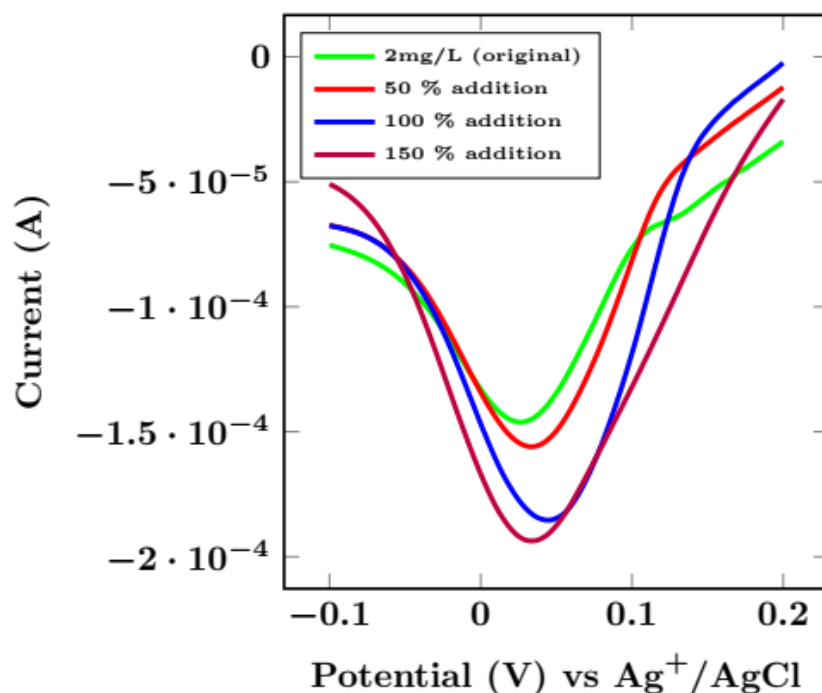
Figure 0.11:Voltammograms of original 2 mg/L phosphate solution spiked with 50%, 100% and 150% of original phosphate concentration.

The peak current increased as spiking increased due to increase in the amount of phosphomolybdate complex.

Table 0.5: Peak currents for original, 50%, 100% and 150% spiking of the original concentration

Concentration	Current (A)
2mg/L (Original)	0.0001464
50% addition	0.0001566
100% addition	0.0001865
150% addition	0.0001939

The percent recovery was computed using Equation 4.10.

$$\% \text{ Recovery} = \frac{\text{Observed Result}}{\text{Expected Result}} \times 100 \qquad (4.10)$$

The observed currents, expected currents (calculated) and percent recoveries at different concentration are given in Table 4.6.

Table 0.6: Percentage Recovery at 50%, 100% and 150% of original phosphate concentration

Concentration	Observed Current (A)	Expected Current(A)	Percent Recovery
2mg/L (original)	0.0001464	0.0001479	99.0 %
50% addition (3mg/L)	0.0001566	0.0001651	94.9 %
100% addition (4mg/L)	0.0001865	0.0001823	102.3 %
150% addition (6mg/L)	0.0001939	0.0002168	89.4 %

The percentage recovery range was found to be between 89% to 102% which was within the recommended limit of 90% to 110% (Thompson, 2002). One possible explanation is that there may have been variability in the sample preparation leading to inconsistent results.

In determination of precision, 10 replicate measurements of 4 mg/L of phosphate were recorded as shown in Figure 4.12.
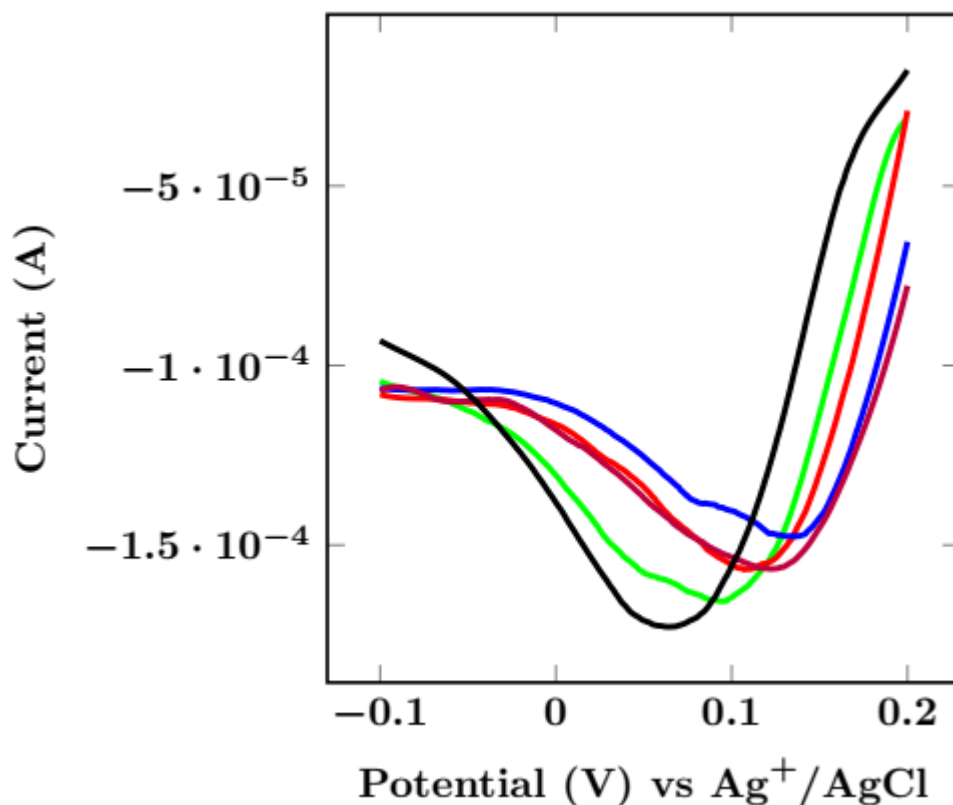
Figure 0.12: Voltammograms of 4 mg/L phosphate concentration.

The precision was calculated using Equation 4.11.

$$\% \, RSD = \frac{s}{\bar{x}} \times 100 \qquad (4.11)$$

The peak currents of 10 replicate measurements were recorded in Table 4.7 below.

Table 0.7: Peak currents of ten replicate measurements of 4 mg/L phosphate concentration.

Run	1	2	3	4	5	6	7	8	9	10
Current x 10^{-3} (A)	1.650	1.581	1.770	1.972	1.675	1.596	1.566	1.587	1.905	1.761

The mean and the standard deviation were determined to be 0.000171 and 0.000014 respectively. Hence, percent RSD was then calculated using Equation 4.11.

$$\% \, RSD = \frac{0.000014}{0.000171} \times 100 = 7.93\%$$

Percent RSD of the ten replicates was found to be 7.93%. Precision provides how well replicate measurements agree with one another and is usually expressed as a standard deviation (Harris, 2010) or the relative standard deviation (Thompson, 2002). The lower the percent RSD the precise the method of analysis i.e., the closer in agreement the obtained results are. For electroanalysis method, a percent RSD of 7.93% is within acceptable limit (usually less 10%) for electroanalysis methods (Gumustas and A. Ozkan, 2011).

4.3.3.1: Phosphomolybdate complex stability.

The standard method for phosphate analysis recommends that absorbance of a sample is read after more than 10 minutes (Murphy and Riley, 1962) after phosphate is reacted by reagents. This is due to oxidation of unreacted ascorbic acid. However, the complex has been reported to be stable for up to 45 minutes (Habibah *et al.*, 2018). A study of the complex stability was also done, so as to determine the time it takes for the complex to form when phosphate is added to the reactants. Figure 4.13 shows voltammograms of 8mg/L of phosphate concentration measured at different duration.
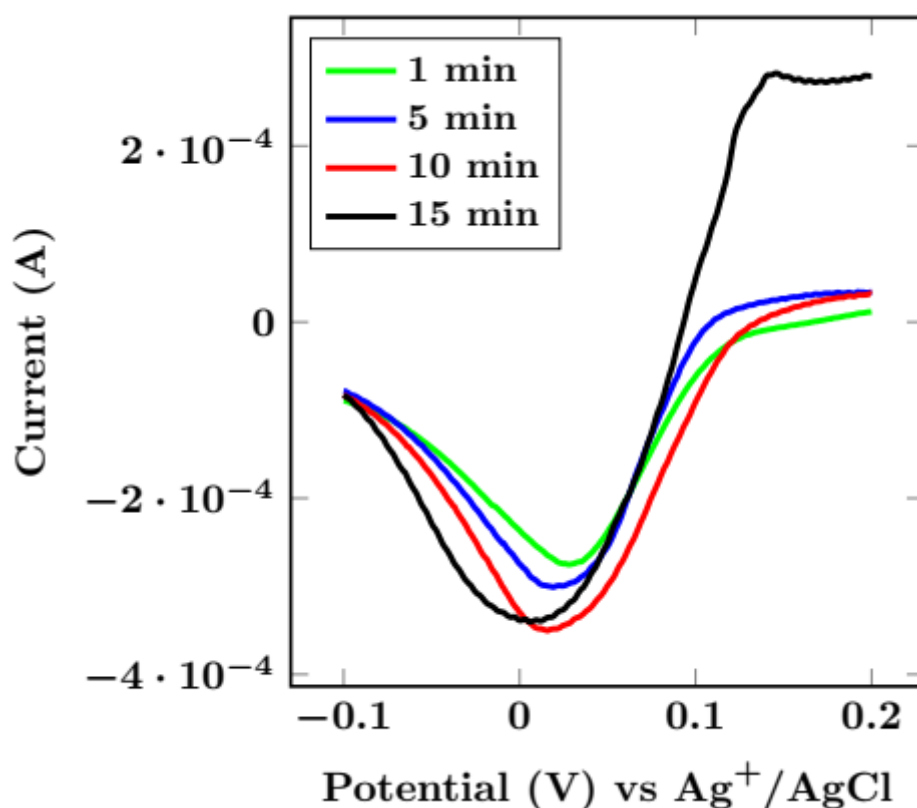
Figure 0.13: Voltammograms recorded after 1, 5, 10, 15 minutes after 8mg/L of phosphate is introduced to the mixed reagent.

59
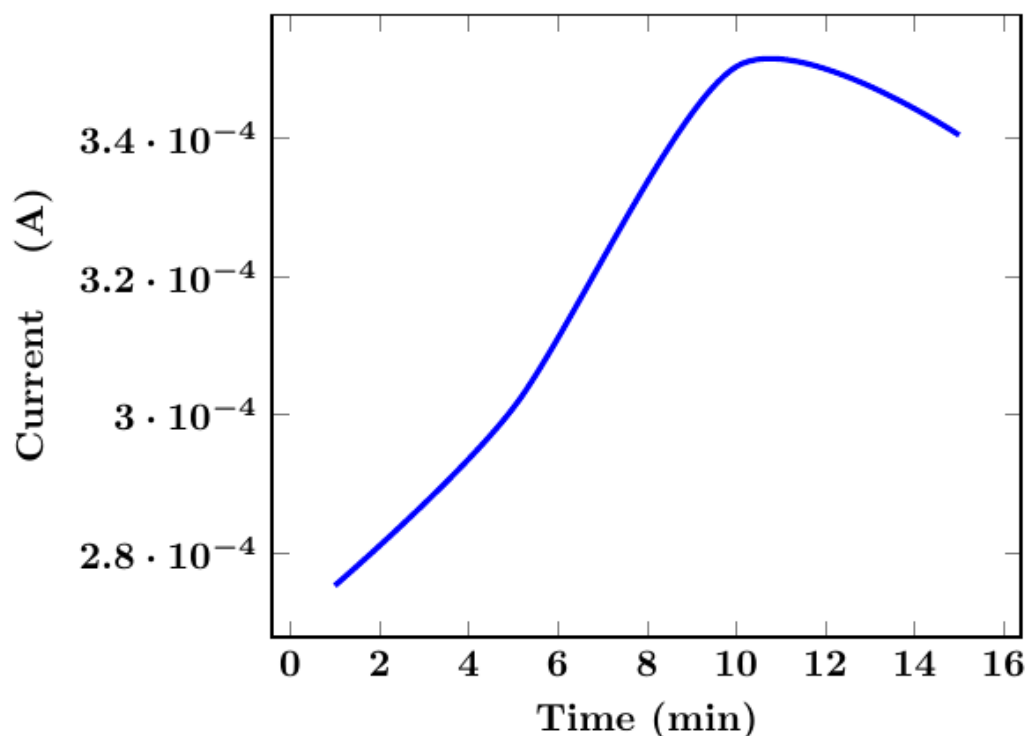
Figure 0.14: DNPV Peak currents of 8 mg/L phosphomolybdate complex against duration of 1, 5, 10 and 15 minutes after introduction of "mixed reagent".

It was noted that the peak was maximum after 10 minutes and then it slightly decreased as shown in Figure 4.14. This indicated that it was necessary to give the complex enough time i.e., 10 minutes before taking measurements because the formation of the complex is not instant. The study indicated that peak current also decreased with increase in time and therefore it was necessary to take measurements not more than 15 minutes after reacting a sample with reagents, this may be attributed to instability of the complex or oxidation of ascorbic acid.

4.4:   Evaluation of DNPV method for determination of phosphates in selected waters.

The Differential Normal Pulse Voltametric method was used to analyse phosphate in natural water obtained from Lake Naivasha, Kenya. Lake Naivasha was chosen because of its eutrophication status which has been witnessed over the decades and continually being monitored (Stoof-Leichsenring *et al.*, 2011; Last and Waithaka, 2017).

Analyses were done on fifty water samples which had been randomly sampled from the lake in a normal wet season. The sample size of fifty was chosen so as to cover a large lake surface. The analysis was done in triplicates and the voltammograms recorded so as to obtain peak

currents of each water sample. Figure 4.15 shows a voltammogram of phosphomolybdate complex from analysing a water sample using DNPV technique.
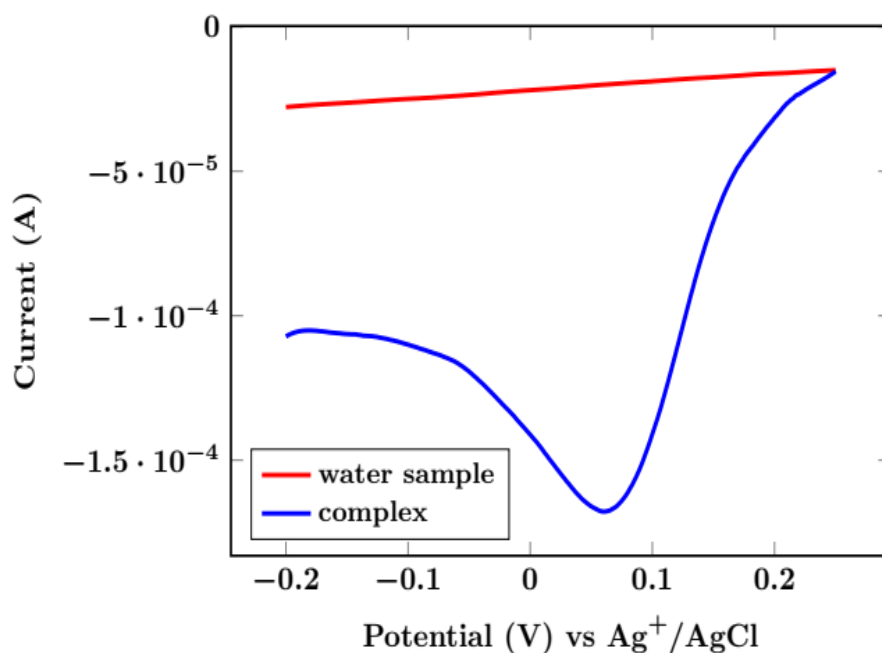
Figure 0.15: Voltammograms of a water sample and that of the phosphomolybdate complex formed after introducing the mixed reagent to the sample

The scan for the natural water sample did not show any peak. However, a peak was observed when the water sample was scanned after adding the reagents. This voltammetric signal was attributed to the formation of the phosphomolybdate complex. The peak observed appeared at 0.06 ± 0.02 V which confirmed a phosphomolybdate complex peak. The peak appearing at 0.06 V was chosen for analyses since it provided a well-defined peak and the peak height could easily be determined.

In order to determine the amount of Phosphate in the samples, phosphate standards of 0, 2, 4, 6 and 8 mg/L were used to prepare a standard calibration curve as shown in Figure 4.17. Phosphate analyses were performed on fifty water samples and the peak currents recorded as shown in Table 4.8.
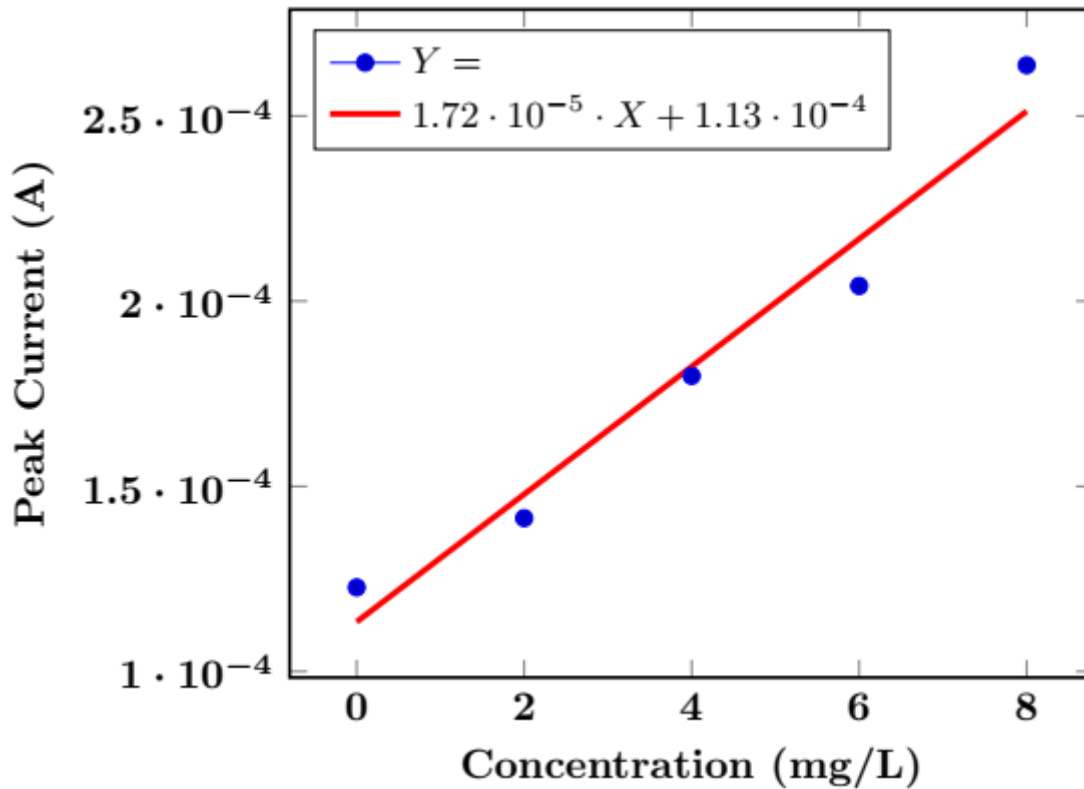
Figure 0.16: Standard calibration curve, peak currents against phosphate concentration, with a linear equation of Y=1.7235·10⁻⁵ X + 0.0001134, and r=0.9816

Phosphate concentration of the water samples were calculated using the equation, $Y = 1.7235 \cdot 10^{-5}\,X + 0.0001134$, as follows.

Rearranging the equation for X, we get Equation 4.12.

$$X = \frac{Y - 0.0001134}{1.7235 \times 10^{-5}} \tag{4.12}$$

Where X is the phosphate concentration and Y is the peak current. For sample 1, phosphate concentration was determined as,

$$X = \frac{0.00012736 - 0.0001134}{1.7235 \times 10^{-5}} = 0.81$$

Similarly, the concentrations of the other samples were also calculated. Table 4.8, provides the peak current and phosphate concentration of fifty water samples.

Table 0.8: Peak currents and phosphate concentration for the 50 water samples

Sample	Peak Current (A)	Phosphate $[PO_4^{3-}]$, Concentration (mg/L)	Sample	Peak Current (A)	Phosphate $[PO_4^{3-}]$, Concentration (mg/L)
1	0.00012736	0.8100	26	0.00013122	1.0339
2	0.00012741	0.8129	27	0.00011919	0.3359
3	0.00010275	0.6179	28	0.0001276	0.8239
4	0.00013286	1.1291	29	0.00013147	1.0484
5	0.00011752	0.2390	30	0.00013163	1.0577
6	0.0001208	0.4294	31	0.00010708	0.3667
7	0.00014339	1.7401	32	0.00012271	0.5402
8	0.00012891	0.8999	33	0.00013005	0.9661
9	0.00011307	0.0191	34	0.00012981	0.9521
10	0.00013522	1.2660	35	0.0001173	0.2263
11	0.0001214	0.4642	36	0.00013034	0.9829
12	0.00011946	0.3516	37	0.00012723	0.8024
13	0.00013045	0.9893	38	0.00010812	0.3064
14	0.00012113	0.4485	39	0.00011702	0.2100
15	0.00012477	0.6597	40	0.0001089	0.2611
16	0.00012008	0.3876	41	0.00012059	0.4172
17	0.00012129	0.4578	42	0.00012591	0.7258
18	0.00011912	0.3319	43	0.00012606	0.7346
19	0.00013004	0.9655	44	0.00012677	0.7757
20	0.0001195	0.3539	45	0.00012072	0.4247
21	0.00011448	0.0627	46	0.00012355	0.5889
22	0.00011308	0.0186	47	0.00011798	0.2657
23	0.00010506	0.4839	48	0.00011061	0.1619
24	0.00010525	0.4729	49	0.00011566	0.1311
25	0.00012602	0.7322	50	0.00013915	1.4941

The mean, $\bar{x}$ and standard deviation s, of the phosphate concentration of the water samples were determined to be 0.6156 mg/L and 0.3811 mg/L respectively.

At 95% confidence level, the confidence limits of the mean concentration were calculated using Equation 4.13.

$$\mu = \bar{x} \pm z \frac{s}{\sqrt{n}} \qquad (4.13)$$

Where $\bar{x}$ the sample mean, s the standard deviation, z is 'z-score', at 95% confidence level $z = 1.96$ and n is the sample size (n = 50).

$$= 0.6156 \pm 1.96 \frac{0.3811}{\sqrt{50}} = 0.6156 \pm 0.1056$$

Therefore, the confidence interval for the mean phosphate concentration was found to range from 0.510 to 0.7212 mg/L. The statistics obtained for the phosphate concentration are summarised and presented in Table 4.9.

Table 0.9: Statistical summary of the phosphate concentration of L. Naivasha water samples

Statistic	Value
Number of samples	50
Minimum	0.0187 mg/L
Maximum	1.7398 mg/L
Mean	0.6156 mg/L
Median	0.5121 mg/L
Variance	0.1452 mg/L
Standard deviation	0.3811 mg/L
95 % confidence interval for the mean	0.510 to 0.7212 mg/L

According to Harper *et al.*, (1993), the concentration of dissolved Phosphorus in lake Naivasha water ranged from 0.3−2 mg/L. A review by Kitaka *et al.,* (2002) on the state of the lake Naivasha with regard to Phosphorus input showed that there was an annual load of 1.4 g/m^2 on the lake surface during wet season and 0.2 g/m^2 in normal wet season. A more recent study by Last and Waithaka, (2017) reported that the average phosphate concentration was 0.33 mg/L.

These studies were based on the phosphomolybdate blue absorbance method to determine phosphate levels in water, however when the developed method (DNPV) was applied, the average phosphate concentration was found to be 0.615 mg/L, with a range of 0.51 to 0.72

mg/L, indicating that the method was able to determine the phosphate level within the same range that had been reported by Harper *et al*., (1993). The elevated phosphate levels observed in the water of Lake Naivasha may be linked to increased human activities, particularly agriculture, in the surrounding region. Agricultural practices, such as the use of fertilizers, can introduce excess nutrients into the lake. This effect may be more pronounced during the wet season when there is an increase in surface runoff that eventually flows into the lake.

CHAPTER FIVE

CONCLUSION AND RECOMMENDATIONS

5.1: Conclusions

A highly sensitive Differential Normal Pulse Voltammetric (DNPV) method for determination of phosphates in water was developed. Assessment of the redox behaviour of phosphomolybdate complex using cyclic voltammetric technique showed two oxidation and two reduction peaks indicating that phosphomolybdate complex is electrochemically active. The DNPV method showed two peaks of the complex which appeared at 0.02 V and at 0.33 V.

The formal redox potentials for the complex were recorded at 0.167 V and 0.357 V while the calculated diffusion coefficients of the redox centres of the complex ware found to be $1.408 \times 10^{-4} \ cm^2 s^{-1}$ and $5.629 \times 10^{-7} \ cm^2 s^{-1}$. The determination of phosphates using DNPV required that the variables be optimized as follows: Amplitude = 0.05V, first and second pulse width = 0.01 seconds, a sampling width = 0.001 seconds, pulse period = 0.001 seconds and a quiet time = 1 second. Further, the study revealed a time frame of 10 minutes to allow complex formation after introducing the reagents and 5 minutes for taking readings, since the complex is unstable after 15 minutes.

The developed method was validated to work in the following parameters. Linear concentration range (LCR), 0 to 8 mg/L of phosphate concentration with a linear correlation coefficient $r = 0.9816$, Limit of detection (LOD) and the Limit of Quantitation (LOQ) of the method were found to be $0.06586 \ mg/L$ and $0.21952 \ mg/L$ respectively. The accuracy of the method in terms of the percentage recovery was in the range of 89% to 102% while the precision in terms percentage relative standard deviation (%RSD) of ten replicate measurements of a single concentration was found to be 7.93%. The accuracy and precision were within acceptable limits.

The method was evaluated by using the natural water from L. Naivasha. DNPV method showed a well-defined peak at 0.06 ± 0.02 V. The method was able to detect phosphate concentrations in 50 water samples and the average concentration was found to be 0.6156±0.1046 mg/L. The study therefore showed that the differential normal pulse voltammetry (DNPV) technique is sensitive enough to analyse phosphate levels in water.

5.2:   Recommendations

The recommendations from this study are:

- Further optimization of the DNPV method by exploring the use of different molybdate salts or oxidizing agents could help to improve its detection limit and enhance its sensitivity for the determination of phosphates in water samples.

- Further research could be conducted on samples of different matrices, e.g., effluents, plant and soil extract especially on interferants that react with molybdate salts to form complexes that would interfere with phosphomolybdate complex analysis.

REFERENCES

Al-Hossainy, A.F., Mohamed, A.E., Hassan, F.S.M. and Abd Allah, M.M. (2017). Determination of cadmium and lead in perch fish samples by differential pulse anodic stripping voltammetry and furnace atomic absorption spectrometry. *Arabian Journal of Chemistry*, **10**: 347–354.

Amare, M. (2019). Voltammetric determination of paracetamol in tablet formulation using Fe (III) doped zeolite-graphite composite modified GCE. *Heliyon*, **5**: 1–6.

Aoki, K., Osteryoung, J. and Osteryoung, R.A. (1980). Differential normal pulse voltammetry-theory. *Journal of Electroanalytical Chemistry and Interfacial Electrochemistry*, **110**: 1–18.

Araujo, P. (2009). Key aspects of analytical method validation and linearity evaluation. *Journal of Chromatography B*, METHOD VALIDATION, COMPARISON AND TRANSFER, **877**: 2224–2234.

Arvía, A.J., Marchiano, S.L. and Podestá, J.J. (1967). The diffusion of ferrocyanide and ferricyanide ions in aqueous solutions of potassium hydroxide. *Electrochimica Acta*, **12**: 259–266.

Baird, R.B., Rice, C.E.W. and Eaton, A.D. (2017). *Standard Methods for the Examination of Water and Wastewater, 23rd. ed.* Water Environment Federation, American Public Health Association , American Water Works Association.

Bakhtiari, M. and Ghalami-Choobar, B. (2015). Thermodynamic study of potassium chloride in glycerol–water mixed solvents using electromotive force measurements at (298.2, 303.2 and 310.2)K. *Journal of Electroanalytical Chemistry*, **754**: 109–117.

Bard, A.J. and Fulkner, L.R. (2000). Polalography and Pulse Voltammetries. In: *Electrochemical Methods Fundamentals and Applications*. Pp. 272, 278. John Wiley & Sons Inc.

Barker, G.C. (1958). Square wave polarography and some related techniques. *Analytica Chimica Acta*, **18**: 118–131.

Batchelor-McAuley, C., Kätelhön, E., Barnes, E.O., Compton, R.G., Laborda, E. and Molina, A. (2015). Recent Advances in Voltammetry. *ChemistryOpen*, **4**: 224–260.

Benitez-Nelson, C.R. (2000). The biogeochemical cycling of phosphorus in marine systems. *Earth Science Reviews*, **51**: 109–135.

Bowes, M.J., Smith, J.T., Jarvie, H.P., Neal, C. and Barden, R. (2009). Changes in point and diffuse source phosphorus inputs to the River Frome (Dorset, UK) from 1966 to 2006. *The Science of the Total Environment*, **407**: 1954–1966.

Campanella, L., Tomassetti, M., D'Ascenzo, G., De Angelis, G., Morabito, R. and Sorrentino, L. (1983). Potentiometric determination of bile phosphates using a lead selective electrode. *Journal of Pharmaceutical and Biomedical Analysis*, **1**: 163–167.

Carter, M., T. and Osteryoung, R.A. (2000). Pulse Voltammetry. In: *Encyclopedia of Analytical Chemistry, Application, Theory and Application*. Pp. 1–23. John Wiley & Sons Ltd.

Chapin, Matson Pamela and Vitousek, Peter M. (2011). Nutrient Cycling. In: *Principles of Terrestrial Ecosystem Ecology*. Pp. 287–290. New York: Springer Science+Business Media.

Christian, G.D., Dasgupta, P.K. and Schug, K. (2014). *Analytical chemistry*. Seventh edition. Hoboken, NJ: John Wiley and Sons, Inc.

Cinti, S., Talarico, D., Palleschi, G., Moscone, D. and Arduini, F. (2016). Novel reagentless paper-based screen-printed electrochemical sensor to detect phosphate. *Analytica Chimica Acta*, **919**: 78–84.

De Marco, R., Clarke, G. and Pejcic, B. (2007). Ion-Selective Electrode Potentiometry in Environmental Analysis. *Electroanalysis*, **19**: 1987–2001.

Dryden, M.D.M. and Wheeler, A.R. (2015). DStat: A Versatile, Open-Source Potentiostat for Electroanalysis and Integration. *PLOS ONE*, 17.

Elgrishi, N., Rountree, K.J., McCarthy, B.D., Rountree, E.S., Eisenhart, T.T. and Dempsey, J.L. (2018). A Practical Beginner's Guide to Cyclic Voltammetry. *Journal of Chemical Education*, **95**: 197–206.

Elizabeth, P. and Victoria, B. (2007). *Quality Assurance in Analytical Chemistry*.

Estefan, Sommer Rolf and John Ryan. (2013). *Methods of Soils, Plant and Water Analysis*. 1st edn. Beirut: ICARDA (International Center for Agricultural Research in the Dry Areas).

Estela, J.M. and Cerdà, V. (2005). Flow analysis techniques for phosphorus: an overview. *Talanta*, **66**: 307–331.

Evard, H., Kruve, A. and Leito, I. (2016). Tutorial on estimating the limit of detection using LC-MS analysis, part II: Practical aspects. *Analytica Chimica Acta*, **942**: 40–49.

Fogg, A.G. and Bsebsu, N.K. (1981). Differential-pulse voltammetric determination of phosphate as molybdovanadophosphate at a glassy carbon electrode and assessment of eluents for the flow injection voltammetric determination of phosphate, silicate, arsenate and germanate. *Analyst*, **106**: 1288–1295.

Fogg, A.G., Bsebsu, N.K. and Birch, B.J. (1981). Differential-pulse anodic voltammetric determination of phosphate, silicate, arsenate and germanate as β-heteropolymolybdates at a stationary glassy-carbon electrode. *Talanta*, **28**: 473–476.

Glazier, S.A. and Arnold, M.A. (1988). Phosphate-selective polymer membrane electrode. *Analytical Chemistry*, **60**: 2540–2542.

Guignard, M.S., Leitch, A.R., Acquisti, C., Eizaguirre, C., Elser, J.J., Hessen, D.O., Jeyasingh, P.D., Neiman, M., Richardson, A.E., Soltis, P.S., Soltis, D.E., Stevens, C.J., Trimmer, M., Weider, L.J., Woodward, G. and Leitch, I.J. (2017). Impacts of Nitrogen and

Phosphorus: From Genomes to Natural Ecosystems and Agriculture. *Frontiers in Ecology and Evolution*, **5**: 1–9.

Gumustas, M. and A. Ozkan, S. (2011). The Role of and the Place of Method Validation in Drug Analysis Using Electroanalytical Techniques. *The Open Analytical Chemistry Journal*, **5**: 1–25.

Gustavo González, A. and Ángeles Herrador, M. (2007). A practical guide to analytical method validation, including measurement uncertainty and accuracy profiles. *TrAC Trends in Analytical Chemistry*, **26**: 227–238.

Habibah, N., Dhyanaputri, I.G.A.S., Karta, I.W., Sundari, C.D.W.H. and Hadi, M.C. (2018). Simple Spectrophotometric Method For The Quantitative Analysis Of Phosphate In The Water Samples. *Jurnal Sains dan Teknolog*, **7**: 198–204.

Harper, D.M., Phillips, G., Chilvers, A., Kitaka, N. and Mavuti, K. (1993). Eutrophication prognosis for Lake Naivasha, Kenya. *SIL Proceedings, 1922-2010*, **25**: 861–865.

Harris, D.C. (2010). *Quantitative chemical analysis*. 8th ed. New York: W.H. Freeman and Co.

Hartmann, J., Moosdorf, N., Lauerwald, R., Hinderer, M. and West, A.J. (2014). Global chemical weathering and associated P-release — The role of lithology, temperature and soil properties. *Chemical Geology*, **363**: 145–163.

Harvey, D. (2011). Analytical Chemistry 2.0—an open-access digital textbook. *Analytical and Bioanalytical Chemistry*, **399**: 149–152.

Hodges, S.C. (2010). Soil fertility basics. *Soil Science Extension, North Carolina State University*.

Inamdar, S.N., Bhat, M.A. and Haram, S.K. (2009). Construction of Ag/AgCl Reference Electrode from Used Felt-Tipped Pen Barrel for Undergraduate Laboratory. *Journal of Chemical Education*, **86**: 355–356.

Jarvie, H.P., Sharpley, A.N., Spears, B., Buda, A.R., May, L. and Kleinman, P.J.A. (2013). Water Quality Remediation Faces Unprecedented Challenges from "Legacy Phosphorus." *Environmental Science & Technology*, **47**: 8997–8998.

Jońca, J., Giraud, W., Barus, C., Comtat, M., Striebig, N., Thouron, D. and Garçon, V. (2013). Reagentless and silicate interference free electrochemical phosphate determination in seawater. *Electrochimica Acta*, **88**: 165–169.

Karube, I., Nomura, Y. and Arikawa, Y. (1995). Biosensors for environmental control. *Trends in Analytical Chemistry*, **14**: 295–299.

Keneth, H. (1990). Phosphorus. In: *Official Methods of Analysis of the Association of Official Analytical Chemists*. P. 342. Virginia USA: Association of Official Analytical Chemists Inc.

Kissinger, P.T. and Heineman, W.R. (1983). Cyclic voltammetry. *Journal of Chemical Education*, **60**: 702–706.

Kitade, T., Kitamura, K., Takegami, S., Miyata, Y., Nagatomo, M., Sakaguchi, T. and Furukawa, M. (2005). Needle-type ultra micro silver/silver chloride reference electrode for use in micro-electrochemistry. *Analytical Sciences: The International Journal of the Japan Society for Analytical Chemistry*, **21**: 907–912.

Kitaka, N., Harper, D.M. and Mavuti, K.M. (2002). Phosphorus inputs to Lake Naivasha, Kenya, from its catchment and the trophic state of the lake. *Hydrobiologia*, **488**: 73–80.

Kolliopoulos, A.V., Kampouris, D.K. and Banks, C.E. (2015). Rapid and Portable Electrochemical Quantification of Phosphorus. *Analytical Chemistry*, **87**: 4269–4274.

Krull, I.S. and Swartz, M. (1999). Analytical Method Development and Validation for the Academic Researcher. *Analytical Letters*, **32**: 1067–1080.

Last, J. and Waithaka, E. (2017). Analysis of some aspects of water quality of Lake Naivasha. *International Journal of Chemical and Life Sciences*, **6**: 2001–2005.

Liang, G., Liu, X. and Li, X. (2013). Highly sensitive detection of α-naphthol based on G-DNA modified gold electrode by electrochemical impedance spectroscopy. *Biosensors and bioelectronics*, **45**: 46–51.

Lovrić, M. and Osteryoung, J. (1982). Theory of differential normal pulse voltammetry. *Electrochimica Acta*, **27**: 963–968.

Macdonald, G.K., Jarvie, H.P., Withers, P.J.A., Doody, D.G., Keeler, B.L., Haygarth, P.M., Johnson, L.T., Mcdowell, R.W., Miyittah, M.K., Powers, S.M., Sharpley, A.N., Shen, J., Smith, D.R., Weintraub, M.N. and Zhang, T. (2016). Guiding phosphorus stewardship for multiple ecosystem services. *Ecosystem Health and Sustainability*, **2**: 1–12.

Martin, P., Van Mooy, B.A.S., Heithoff, A. and Dyhrman, S.T. (2011). Phosphorus supply drives rapid turnover of membrane phospholipids in the diatom Thalassiosira pseudonana. *The ISME journal*, **5**: 1057–1060.

Miedlich, S.U., Zalutskaya, A., Zhu, E.D. and Demay, M.B. (2010). Phosphate-induced Apoptosis of Hypertrophic Chondrocytes Is Associated with a Decrease in Mitochondrial Membrane Potential and Is Dependent upon Erk1/2 Phosphorylation. *The Journal of Biological Chemistry*, **285**: 18270–18275.

Miller, J.N. and Miller, J.C. (2010a). *Statistics and chemometrics for analytical chemistry*. 6. ed. Harlow: Prentice Hall.

Miller, J.N. and Miller, J.C. (2010b). Statistics and Chemometrics for Analytical Chemistry, 6th Edition.

Mitra, S. (2004). *Sample Preparation Techniques in Analytical Chemistry*. John Wiley & Sons.

Mogollón, J.M., Beusen, A.H.W., Grinsven, H.J.M. van, Westhoek, H. and Bouwman, A.F. (2018). Future agricultural phosphorus demand according to the shared socioeconomic pathways. *Global Environmental Change*, **50**: 149–163.

Molina, Á. and González, J. (2016). Double Pulse Voltammetries. In: *Pulse Voltammetry in Physical Electrochemistry and Electroanalysis: Theory and Applications*, Monographs in Electrochemistry (edited by Á. Molina & J. González). Pp. 229–316. Cham: Springer International Publishing.

Molina, A., Moreno, M.M., Serna, C. and Camacho, L. (2001). Additive differential pulse voltammetry, instead of double differential pulse voltammetry. *Electrochemistry Communications*, **3**: 324–329.

Murphy, J. and Riley, J.P. (1962). A modified single solution method for the determination of phosphate in natural waters. *Analytica Chimica Acta*, **27**: 31–36.

Neves, M.S.A.C., Souto, M.R.S., Tóth, I.V., Victal, S.M.A., Drumond, M.C. and Rangel, A.O.S.S. (2008). Spectrophotometric flow system using vanadomolybdophosphate detection chemistry and a liquid waveguide capillary cell for the determination of phosphate with improved sensitivity in surface and ground water samples. *Talanta*, 14th International Conference on Flow Injection Analysis and Related Techniques, **77**: 527–532.

Osteryoung, R.A., Osteryoung, J., Albery, W.J., Rogers, G.T., Feilden, G.B.R., Rogers, G.T. and Albery, W.J. (1981). Pulse voltammetric methods of analysis. *Philosophical Transactions of the Royal Society of London. Series A, Mathematical and Physical Sciences*, **302**: 315–326.

Parry, E.P. and Osteryoung, R.A. (1965). Evaluation of Analytical Pulse Polarography. *Analytical Chemistry*, **37**: 1634–1637.

Patey, M.D., Rijkenberg, M.J.A., Statham, P.J., Stinchcombe, M.C., Achterberg, E.P. and Mowlem, M. (2008). Determination of nitrate and phosphate in seawater at nanomolar concentrations. *TrAC Trends in Analytical Chemistry*, **27**: 169–182.

Penner, M.H. (2017). Basic Principles of Spectroscopy. In: *Food Analysis* (edited by S.S. Nielsen). Pp. 79–88. Cham: Springer International Publishing.

Peters, F.T., Drummer, O.H. and Musshoff, F. (2007). Validation of new methods. *Forensic Science International*, Research in Forensic Medicine and Forensic Sciences: Basic Principles and Application in Practice, **165**: 216–224.

Pletcher, D., Greef, R., Robinson, J., Petere, L.M. and Robinson, J. (2011). *Instrumental Methods in Electochemistry*. 5th edn. Philadelphia: Woodhead Publishing Limited.

Pradyot, Patnaik. (2018). Phosphorus. In: *Handbook of Environmental Analysis Chemical Pollutants in Air, Water, Soil, and Solid Wastes*. Pp. 281–284. Boca Raton: Taylor & Francis Group, LLC.

Radu, A. and Diamond, D. (2007). Chapter 2 Ion-selective electrodes in trace level analysis of heavy metals: Potentiometry for the XXI century. In: *Comprehensive Analytical Chemistry*, Electrochemical Sensor Analysis (edited by S. Alegret & A. Merkoçi). Pp. 25–52. Elsevier.

Schindler, D.W. (1971). Carbon, Nitrogen, and Phosphorus and the Eutrophication of Freshwater Lakes1. *Journal of Phycology*, **7**: 321–329.

Schindler, D.W., Carpenter, S.R., Chapra, S.C., Hecky, R.E. and Orihel, D.M. (2016). Reducing Phosphorus to Curb Lake Eutrophication is a Success. *Environmental Science & Technology*, **50**: 8923–8929.

Sharpley, A.N., Bergström, L., Aronsson, H., Bechmann, M., Bolster, C.H., Börling, K., Djodjic, F., Jarvie, H.P., Schoumans, O.F., Stamm, C., Tonderski, K.S., Ulén, B., Uusitalo, R. and Withers, P.J.A. (2015). Future agriculture with minimized phosphorus losses to waters: Research needs and direction. *AMBIO*, **44**: 163–179.

Shrivastava, A. and Gupta, V.B. (2011). Methods for the determination of limit of detection and limit of quantitation of the analytical methods. *Chronicles of young scientists*, **2**: 21–25.

Skoog, D.A., Holler, F.J. and Crouch, S.R. (2017). *Principles of Instrumental Analysis*. Boston: Cengage Learning.

Skoog, D.A., West, D.M., Holler, F.J. and Crouch, S.R. (2013). *Fundamentals of Analytical Chemistry*. Belmont: Cengage Learning.

Son, J.-H., Ohlin, C.A., Johnson, R.L., Yu, P. and Casey, W.H. (2013). A Soluble Phosphorus-Centered Keggin Polyoxoniobate with Bicapping Vanadyl Groups. *Chemistry – A European Journal*, **19**: 5191–5197.

Song, H. and Cabooter, D. (2017). Relevance and Assessment of Molecular Diffusion Coefficients in Liquid Chromatography. *Chromatographia*, **80**: 651–663.

Song, Y., Bian, C., Li, Y., Tong, J. and Xia, S. (2016). Electrochemical Determination of Phosphate in Freshwater Free of Silicate Interference. *Journal of Biomedical Sciences*, **5**: 1–6.

Stojek, Z. (2010). Pulse Voltammetry. In: *Electroanalytical Methods: Guide to Experiments and Applications* (edited by F. Scholz, A.M. Bond, R.G. Compton, D.A. Fiedler, G. Inzelt, H. Kahlert, Š. Komorsky-Lovrić, H. Lohse, M. Lovrić, F. Marken, A. Neudeck, U. Retter, F. Scholz & Z. Stojek). Pp. 107–119. Berlin, Heidelberg: Springer Berlin Heidelberg.

Stoof-Leichsenring, K.R., Junginger, A., Olaka, L.A., Tiedemann, R. and Trauth, M.H. (2011). Environmental variability in Lake Naivasha, Kenya, over the last two centuries. *Journal of Paleolimnology*, **45**: 353–367.

Taverniers, I., Van Bockstaele, E. and De Loose, M. (2010). Analytical Method Validation and Quality Assurance. In: *Pharmaceutical Sciences Encyclopedia*. Pp. 1–48. John Wiley & Sons, Ltd.

Taylor, J.K. (1983). Validation of analytical methods. *Analytical Chemistry*, **55**: 600–608.

Thompson, M.L. and Kateley, L.J. (1999). The Nernst Equation: Determination of Equilibrium Constants for Complex Ions of Silver. *Journal of Chemical Education*, **76**: 95–96.

Thompson, R. (2002). Harmonized Guidelines for Single- Laboratory Validation of Methods of Analysis (IUPAC Technical Report). *Chemistry International -- Newsmagazine for IUPAC*, **24**: 26–26.

Tomková, H., Sokolová, R., Opletal, T., Kučerová, P., Kučera, L., Součková, J., Skopalová, J. and Barták, P. (2018). Electrochemical sensor based on phospholipid modified glassy carbon electrode - determination of paraquat. *Journal of Electroanalytical Chemistry*, Modern Electrochemical Methods XXXVII, **821**: 33–39.

Torrezani, L., Saczk, A.A., Firmino de Oliveira, M., Stradiotto, N.R. and Okumura, L.L. (2011). Voltammetric Determination of Phosphate in Brazilian Biodiesel Using Two Different Electrodes. *Electroanalysis*, **23**: 2456–2461.

Urasa, I.T. and Ferede, F. (1986). The Determination of Phosphates using Ion Chromatography: An Evaluation of Influential Factors. *International Journal of Environmental Analytical Chemistry*, **23**: 189–206.

Villalba, M.M., McKeegan, K.J., Vaughan, D.H., Cardosi, M.F. and Davis, J. (2009). Bioelectroanalytical determination of phosphate: A review. *Journal of Molecular Catalysis B: Enzymatic*, **59**: 1–8.

Wang, F., Tong, J., Li, Y., Bian, C., Sun, J. and Xia, S. (2014). An Electrochemical Microsensor Based on a AuNPs-Modified Microband Array Electrode for Phosphate Determination in Fresh Water Samples †. *Sensors (Basel, Switzerland)*, **14**: 24472–24482.

Wang, J. (2000). *Analytical Electrochemistry (Second Edition)*. Erscheinungsort nicht ermittelbar: Wiley-VCH.

Wang, J. (2004). *Analytical Electrochemistry*. John Wiley & Sons.

Willard, H.H., Merritt, L.L.Jr., Dean, J.A. and Settle, F.A.Jr. (1988). *Instrumental methods of analysis, 7th edition*. United States: Wadsworth Publishing Company.

Withers, P.J.A., Neal, C., Jarvie, H.P. and Doody, D.G. (2014). Agriculture and Eutrophication: Where Do We Go from Here? *Sustainability*, **6**: 5853–5875.

Worsfold, P., McKelvie, I. and Monbet, P. (2016). Determination of phosphorus in natural waters: A historical review. *Analytica Chimica Acta*, **918**: 8–20.

Wu, W., Jia, M., Zhang, Z., Chen, X., Zhang, Q., Zhang, W., Li, P. and Chen, L. (2019). Sensitive, selective and simultaneous electrochemical detection of multiple heavy metals in environment and food using a lowcost Fe3O4 nanoparticles/fluorinated multi-walled carbon nanotubes sensor. *Ecotoxicology and Environmental Safety*, **175**: 243–250.

Wurtsbaugh, W.A., Paerl, H.W. and Dodds, W.K. (2019). Nutrients, eutrophication and harmful algal blooms along the freshwater to marine continuum. *WIREs Water*, **6**: e1373.

Zare, H.R. and Nasirizadeh, N. (2010). Simultaneous determination of ascorbic acid, adrenaline and uric acid at a hematoxylin multi-wall carbon nanotube modified glassy carbon electrode. *Sensors and Actuators B: Chemical*, **143**: 666–672.

Zhang, S., Wang, N., Yu, H., Niu, Y. and Sun, C. (2005). Covalent attachment of glucose oxidase to an Au electrode modified with gold nanoparticles for use as glucose biosensor. *Bioelectrochemistry*, **67**: 15–22.

Zhu, Y., Li, C., Wang, L., Chen, M., Yu, J., Liu, Q. and Chen, X. (2019). Differential Pulse Voltammetry Determination of Ofloxacin in Human Serum and Urine Based on a Novel Tryptophan-graphene Oxide-carbon Nanotube Electrochemical Sensor. *Electroanalysis*, **31**: 1429–1436.

Zuman, P. (2001). Electrolysis with a Dropping Mercury Electrode: J. Heyrovsky's Contribution to Electrochemistry. *Critical Reviews in Analytical Chemistry*, **31**: 281–289.